polymers

MDPI

Article

From Waste to Ship Materials: Development and Performance of Recycled Polymer Composites for Sustainable Maritime Applications

Ömer Şengül [1,*], Murat Yorulmaz [2] and İdris Karagöz [3,4,*]

[1] Department of Maritime Transportation and Management Engineering, Maritime Faculty, Kocaeli University, Kocaeli 41500, Türkiye
[2] Department of Maritime Busineess Management, Maritime Faculty, Kocaeli University, Kocaeli 41500, Türkiye; murat.yorulmaz@kocaeli.edu.tr
[3] Department of Polymer Materials Engineering, Faculty of Engineering, Yalova University, Yalova 77200, Türkiye
[4] Zamia Composite Research and Development Technology Joint Stock Company, ULUTEK Technopark, Nilüfer 16110, Türkiye
* Correspondence: omer.sengul@kocaeli.edu.tr (Ö.Ş.); idris.karagoz@yalova.edu.tr (İ.K.)

Abstract

This study investigates the potential of cone powder (PCP) as a sustainable filler in recycled polypropylene (rPP) composites for marine-related applications. Composites containing 5–20 wt.% PCP were manufactured by twin-screw extrusion and injection molding and characterized in terms of mechanical, thermal, chemical, morphological, and seawater absorption properties. At 20 wt.% PCP, flexural modulus and strength increased by 49.4% and 38.7%, respectively, compared with unfilled rPP. Tensile strength increased from 15.65 to 16.63 MPa, whereas impact strength decreased by 59.2% and elongation at break declined from 93.9% to 19.5%, indicating a stiffness–toughness trade-off. FTIR analysis identified characteristic lignocellulosic functional groups, while DSC revealed distinct melting transitions. TGA showed variations in initial degradation behavior, with principal degradation peaks remaining between 482.8 and 485.0 °C. After 960 h (40 days) of natural seawater immersion, absorption increased from 0.2005% for unfilled rPP to 1.1356% for the 20 wt.% PCP composite. Overall, PCP-containing rPP composites exhibited improved flexural performance but reduced impact resistance and increased moisture uptake. These findings suggest potential applications in selected marine-related components where stiffness is prioritized, although long-term durability and mechanical property retention after seawater exposure require further investigation.

Keywords: recycled polypropylene; cone powder; lignocellulosic waste; polymer composites; seawater absorption; marine applications

Check for updates

Academic Editor: Helena Felgueiras

Received: 12 October 2026
Revised: 17 November 2026
Accepted: 20 November 2026
Published: 24 November 2026

Copyright: © 2026 by the authors. Licensee MDPI, Basel, Switzerland. This article is an open access article distributed under the terms and conditions of the Creative Commons Attribution (CC BY) license.

1. Introduction

Traditional composite materials widely used in the maritime sector—particularly glass-fibre-reinforced plastics—pose significant sustainability challenges due to their high environmental impact, limited recycling potential and the long-term waste problems they cause at the end of their service life. In contrast, recycled polymers and natural fillers offer more environmentally sustainable alternatives to traditional composite materials. However, the competitiveness of these materials compared to traditional composites in terms of mechanical strength, water absorption behaviors, resistance to marine environment

conditions and long-term performance has not yet been sufficiently and comprehensively demonstrated. In this context, it is important to ensure that recycled polymer-based composites, reinforced with natural fillers, are endowed with properties capable of meeting the mechanical, physical and environmental performance criteria required by maritime applications. Technological developments and innovative practices are also gaining increasing importance in the maritime sector [1].

The growing accumulation of plastic waste and the continued consumption of fossil resources have intensified efforts to develop materials within a circular economy framework. In this context, the adoption of sustainable production practices is becoming increasingly important across various industrial sectors. Mechanical recycling offers a practical route for extending the service life of PP and reducing the demand for virgin polymer; however, repeated processing and previous service exposure may induce thermo-oxidative degradation, chain scission, and structural changes, ultimately affecting the mechanical and rheological performance of recycled polypropylene (rPP) [2,3]. Consequently, improving performance and broadening the potential applications of rPP remain important challenges in the development of more sustainable polymer systems.

One promising strategy is the incorporation of lignocellulosic residues into recycled thermoplastics. Agricultural and forestry-derived residues can serve as low-density, renewable fillers while simultaneously reducing polymer consumption and providing value-added pathways for biomass streams that might otherwise be discarded or used in low-value applications [1,4,5]. The combination of recycled polymers with waste-derived lignocellulosic fillers is particularly attractive because it addresses two waste streams within the same material system. Previous studies have demonstrated the feasibility of incorporating rice husk, rubberwood flour, kenaf, sisal, and other plant-derived fillers into rPP matrices [4–8]. Depending on filler type, concentration, particle morphology, processing conditions, and interfacial adhesion, these materials commonly exhibit increased stiffness, whereas tensile strength, ductility, impact resistance, and moisture sensitivity may vary considerably [4–8]. These findings highlight the need to evaluate individual biomass sources rather than assuming equivalent behavior among lignocellulosic fillers.

Pine cones represent an interesting lignocellulosic resource for this purpose. They are generated as forest biomass and remain comparatively underutilized despite containing substantial fractions of structural lignocellulosic components. Pine cone biomass has been reported to contain a considerable cellulose fraction, together with hemicellulose and lignin, supporting its potential as a source of reinforcement or particulate filler for composite materials [9]. In addition, pine cones contain extractives that can influence interfacial and processing behavior when incorporated into polymer matrices [10]. The utilization of pine cone residues as composite constituents may therefore provide an alternative valorization route for this biomass while reducing the fraction of petroleum-derived polymer required in the final material. Previous investigations have demonstrated the potential of pine cone-derived fibers or flour in PP-based composites. Arrakhiz et al. [11], for example, reported that compatibilized pine cone fiber/PP composites exhibited substantial increases in Young's modulus, although the incorporation of lignocellulosic fibers affected thermal degradation behavior. Similarly, pine cone scale fibers have been successfully incorporated into PP-based hybrid composites, with changes in tensile, flexural, impact, hardness, and morphological characteristics depending on formulation [12]. Earlier work using pine cone flour in wood/PP composites also showed that increasing cone flour content can influence both flexural properties and water resistance, demonstrate the importance of filler concentration when design such materials [13].

A major challenge associated with lignocellulosic filler/polyolefin composites arises from the dissimilar surface chemistry of the two constituents. Hydroxyl-rich lignocellulosic

surfaces are relatively hydrophilic, whereas PP is non-polar and hydrophobic, which can result in insufficient wetting, poor filler dispersion, interfacial voids, and inefficient stress transfer [6,14]. These effects may become increasingly pronounced as filler content increases and can contribute to reductions in strength and ductility as well as increased moisture uptake. Maleic-anhydride-grafted polypropylene (PP-g-MA or MAPP) is therefore widely employed to improve compatibility between PP and lignocellulosic fillers. Maleic anhydride functionalities can interact with hydroxyl-containing groups on the filler surface while the polypropylene backbone remains compatible with the matrix, thereby improving interfacial adhesion [5,6,14]. For rPP-based systems, improved compatibility is particularly relevant because the properties of the recycled matrix may already have been altered by previous processing and degradation. Recent work on rPP/rice-husk composites, for example, demonstrated that PP-g-MA and particle size significantly affected interfacial adhesion, morphology, flow behavior, and mechanical performance [15].

More specifically, recent investigations have established that cone powder (PCP) can interact beneficially with recycled PP. Do et al. [2] incorporated PCP into repeatedly processed rPP and reported that a formulation containing 15 wt.% PCP increased tensile strength from 21.17 to 25.86 MPa and flexural strength from 35.2 to 43.75 MPa relative to the corresponding rPP, while also improving thermal stability. Nevertheless, non-uniform particle dimensions and local interfacial debonding indicated that filler dispersion and interfacial quality remained important controlling factors [2]. A subsequent study demonstrated that cone powder could also affect the crystallization behavior of recycled PP, with 15 wt.% PCP promoting β-phase crystallization and producing improvements in toughness, impact behavior, tensile strength, and flexural modulus [3]. These observations suggest that pine cone particles should not be regarded merely as an inert replacement for polymer; rather, they may influence morphology, crystallization, stress transfer, and resulting macroscopic properties of rPP. Particle size and surface condition are likewise important: Singh et al. [16] reported improved mechanical performance when finer and alkali-treated pine cone particles were incorporated into recycled thermoplastic composites.

Despite these promising findings, the available literature remains relatively limited compared with that for conventional lignocellulosic fillers, and important questions remain concerning the systematic relationship between pine cone loading and the overall performance profile of rPP-based composites. Existing studies have primarily focused on specific reinforcement configurations, surface treatments, hybrid polymer systems, repeated-recycling behavior, or selected mechanical properties [2,3,11–13,16]. For example, PP/PLA/pine cone flour systems have demonstrated that filler loading, PP-g-MA compatibilization, and surface treatment can substantially affect crystallization, thermal stability, impact behavior, and water absorption [17], further emphasizing that pine cone concentration and interface characteristics must be considered together. Nevertheless, a systematic assessment combining the mechanical, thermal, and physical responses of pine cone-filled recycled PP across a controlled range of filler contents remains valuable for establishing structure–property relationships and defining practical formulation windows.

Although Kabache et al. [17] investigated the effects of compatibilization on pine cone flour-reinforced PP/PLA blends, and Do et al. [2] demonstrated the mechanical reinforcement potential of PCP in recycled polypropylene, the present study addresses a different research objective. Specifically, it evaluates the combined mechanical, thermal, morphological, and short-term natural seawater absorption responses of PCP-containing recycled polymer composites across filler concentrations of 5–20 wt.%. Unlike studies primarily emphasizing reinforcement efficiency or compatibilization, the present investigation highlights the concentration-dependent trade-offs among flexural strength, impact resistance, thermal

stability, and seawater absorption, providing a more comprehensive basis for evaluating the potential and limitations of these recycled composites in marine-related applications.

Accordingly, the present study investigates the valorization of pine cone waste as a lignocellulosic filler in recycled polypropylene composites. Cone powder was incorporated into an rPP matrix at different loading levels, and the resulting composites were systematically characterized in terms of their mechanical, thermal, and physical properties. Particular attention was given to the influence of pine cone content on stiffness, strength, toughness, thermal behavior, and water-related properties in order to identify the balance between increased biomass utilization and preservation of functional performance. By combining a recycled thermoplastic matrix with an underutilized forestry-derived residue, this work seeks to contribute to the development of resource-efficient composite materials and to assess their potential for non-structural applications, including components intended for humid or marine-related service environments.

2. Materials and Methods

2.1. Materials and Composite Formulations

A recycled polyolefin material, identified as recycled polypropylene (rPP) by the recycling supplier, was obtained from the Polymer Processing Laboratory of Yalova University (Yalova, Türkiye). According to the supplier's technical data sheet, the rPP had a melt flow rate (MFR) of 5.9 g/10 min at 230 °C/2.16 kg, a density of 0.905 g/cm^3, and a melting point of 162 °C.

Cones of *Arceuthos drupacea* (syn. *Juniperus drupacea*) were collected from Kahramanmaraş, southeastern Türkiye, and used as the lignocellulosic filler. The collected cones were ground and subsequently sieved, and the fraction with a particle size below 100 µm was used as cone powder in the composite formulations. Prior to melt compounding, the sieved PCP was oven-dried at 100 °C for 4 h to reduce its moisture content. The use of a defined particle-size fraction and standardized drying conditions was intended to minimize preparation-related variability. The chemical composition of *Arceuthos drupacea* cones has previously been investigated by Dönmez et al. [18], who reported holocellulose and α-cellulose contents of 40.36 and 28.81 wt.%, respectively, and a Klason lignin content of 32.20 wt.%. The chemical composition of the PCP used in the present study was also characterized to enable comparison with the literature-reported values, as described in Section 2.2.

Maleic-anhydride-grafted polypropylene (PP-g-MA; Olebond 7401 HH, Tisan Engineering Plastics, Istanbul, Türkiye) was used as a compatibilizer. Olebond 7401 HH has a density of 0.93 g/cm^3, an MFR above 100 g/10 min (230 °C/2.16 kg), and a melting point of 162 °C. Its maleic anhydride grafting level is specified by the manufacturer as high (0.5–1%). Irganox 1010 and Irgafos 168 (BASF) were used as the primary antioxidant and processing stabilizer, respectively, while polyethylene (PE) wax was incorporated as a processing lubricant.

Five formulations were prepared, consisting of a stabilized rPP control and rPP composites containing 5, 10, 15, and 20 wt.% PCP. The concentrations of Irganox 1010, Irgafos 168, and PE wax were maintained at 0.10, 0.10, and 0.25 wt.%, respectively, in all formulations. PP-g-MA was incorporated at a constant concentration of 3 wt.% in all PCP-containing composites to promote interfacial compatibility between PCP and the rPP matrix while maintaining a constant compatibilizer concentration across the filled formulations. The maleic anhydride functionalities of PP-g-MA may interact with hydroxyl groups present in the lignocellulosic constituents of PCP, while its polypropylene backbone promotes compatibility with the polyolefin matrix. The compatibilizer concentration was kept constant to evaluate the influence of PCP loading without introducing an additional formulation

variable. The unfilled rPP control did not contain PP-g-MA; therefore, comparisons with this control reflect the overall effects of the compatibilized composite formulations rather than the independent effect of PCP. The rPP content was adjusted accordingly to maintain a total formulation of 100 wt.%. The compositions and sample codes are summarized in Table 1. The fixed PP-g-MA concentration (3 wt.%) across all PCP-containing formulations enabled the evaluation of PCP loading effects within a consistently compatibilized rPP composite system.

Table 1. Composition of the investigated rPP-based composites.

Sample Code	rPP (wt.%)	Cone Powder (wt.%)	Irganox 1010 (wt. %)	Irgafos 168 (wt.%)	PP-g-MA (wt.%)	PE Wax (wt.%)
rPP(Control)	99.55	-	0.10	0.10	-	0.25
rPP-PCP5	91.55	5	0.10	0.10	3	0.25
rPP-PCP10	86.55	10	0.10	0.10	3	0.25
rPP-PCP15	81.55	15	0.10	0.10	3	0.25
rPP-PCP20	76.55	20	0.10	0.10	3	0.25

2.2. Preparation and Characterization of Cone Powder and Composite Specimens

The chemical composition of *Arceuthos drupacea* cone powder was determined to quantify its ash, extractive, cellulose, hemicellulose, and lignin contents. Ash content was determined according to ASTM D1102 [19], while holocellulose content was measured using the Wise method based on acidified sodium chlorite treatment. Extractive content was determined by benzene–ethanol solvent extraction, following Li et al. [20]. Hemicellulose content was determined by alkaline extraction of extractive-free samples. Lignin content was determined using the Klason method in accordance with ASTM D1106-21 [21] and TAPPI T 222 om-21 [22]. Cellulose content was calculated indirectly using a mass-balance approach, as described in previous studies [20,23,24]. All analyses were performed in triplicate, and the results were expressed as mean ± standard deviation.

The constituents of each formulation listed in Table 1 were weighed according to their respective mass fractions and premixed to ensure a uniform distribution of PCP and additives within the rPP matrix. Following premixing, the formulations were processed in a GS25 co-rotating twin-screw extruder (GS Mach Equipment Co. Ltd., Nanjing, China) with a screw diameter of 21.6 mm. Compounding was performed at a constant screw rotation rate of 300 rpm. The seven heating zones along the barrel were adjusted sequentially to 150, 160, 170, 180, 190, 200, and 210 °C from the feed zone to the die. After exiting the die, the continuous extrudate was cooled and converted into pellets for subsequent injection molding. Before injection molding, the compounded pellets were dried at 60 °C for 2 h to minimize residual moisture.

Standard test specimens were produced from the dried pellets using an Engel Victory 400 Tech injection molding machine (ENGEL Austria GmbH, Schwertberg, Austria). The temperature settings from the rear barrel zone toward the nozzle were 175, 185, 195, 205, and 210 °C, respectively. During molding, the mold temperature was maintained at 40 ± 5 °C. An injection pressure of 80 bar, an injection speed of 50 mm s^{-1}, and a holding pressure of 55 bar were applied, with a total molding cycle time of 35 s. Identical injection-molding conditions were employed for the rPP control and all PCP-containing composites to ensure consistent processing conditions across the investigated formulations. The preparation route of PCP and the subsequent production of the rPP/PCP composite specimens are schematically illustrated in Figure 1.

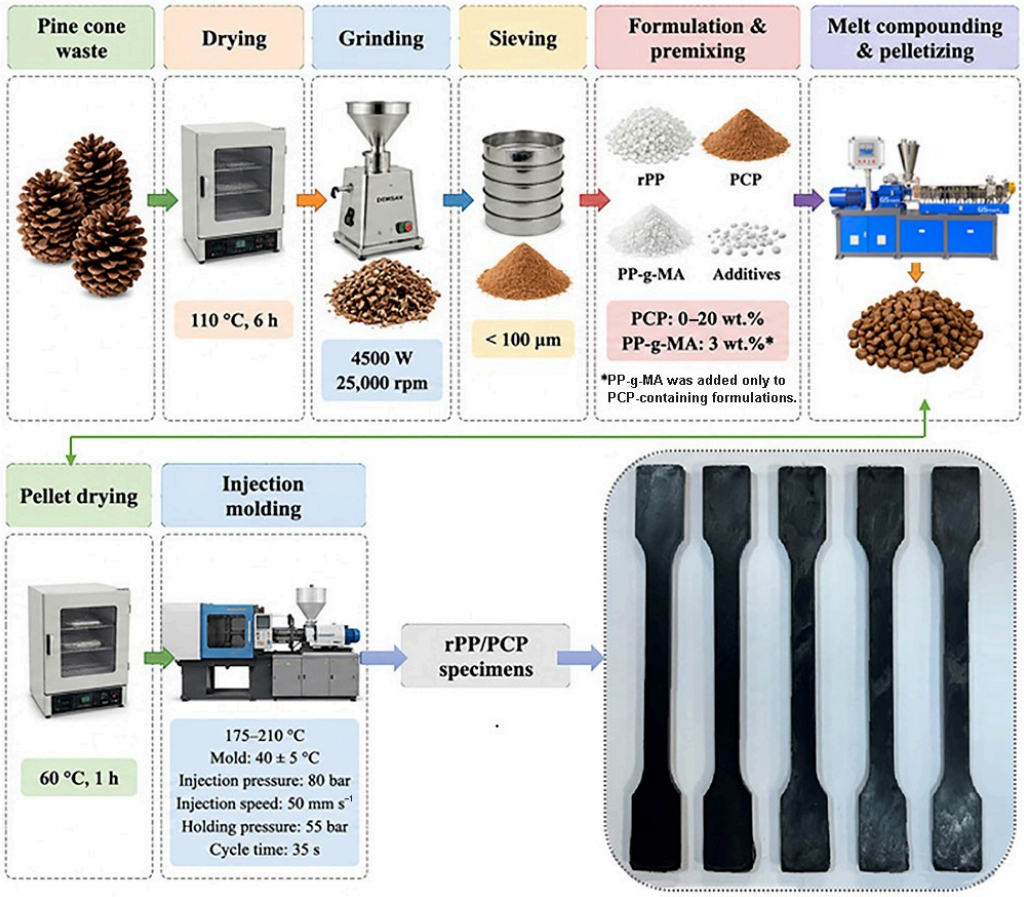

Figure 1. Representative injection-molded specimens of the rPP/PCP composites with different cone powder contents.

2.3. Mechanical Characterization

The mechanical performance of the rPP/PCP composites was evaluated through tensile, flexural, impact, and hardness measurements. All tests were carried out under ambient laboratory conditions.

Tensile properties were determined according to ISO 527-1 [25] using a Zwick Z020 universal testing system (ZwickRoell GmbH & Co. KG, Ulm, Germany) fitted with a 20 kN load cell. The specimens were loaded at a crosshead displacement rate of 50 mm min^{-1}. Five specimens were evaluated for each formulation.

Flexural behavior was assessed by three-point bending in accordance with ISO 178 [26]. Measurements were performed using the same Zwick Z020 testing system at a crosshead speed of 1.7 mm min^{-1}. Five replicate specimens were examined for each formulation.

V-notched Izod impact tests were conducted according to ISO 180 [27] using an Instron 120D impact testing machine (Instron, Norwood, MA, USA) equipped with a 7.5 J pendulum. Ten specimens were tested for each formulation, and the mean impact strength was calculated from the individual measurements.

Shore D hardness was measured using a Loyka M01D analog durometer (Loyka, Istanbul, Türkiye) in accordance with ISO 868 [28]. Five independently prepared specimens were evaluated for each formulation, with one measurement obtained from each specimen ($n = 5$).

2.4. Short-Term Seawater Absorption

The seawater absorption behavior of the rPP/PCP composites was investigated using specimens measuring 4 × 20 × 30 mm. Natural seawater used in the experiment was collected

from the Marmara Sea in Koru, Yalova, Türkiye. For each formulation, three independently prepared specimens were tested ($n = 3$). Prior to immersion, the specimens were dried to minimize residual moisture and weighed to determine their initial dry mass (m_0).

The specimens were fully immersed in seawater in separate sealed containers for each formulation and maintained at 23 °C for 960 h (40 days). An identical seawater-to-specimen ratio was maintained across all formulations to ensure comparable exposure conditions. Changes in specimen mass were monitored at predetermined intervals throughout the immersion period. At each measurement interval, the specimens were removed from the seawater, gently blotted to eliminate excess surface moisture, and immediately weighed. Following weighing, the specimens were returned to their respective containers to continue immersion. The same seawater was retained throughout the experiment without replacement.

Seawater absorption was determined from the relative change in specimen mass using Equation (1):

$$WA(\%) = \left(\frac{m_t - m_0}{m_0}\right) \quad (1)$$

where m_0 is the initial dry mass of the specimen and m_t represents its mass after an immersion time of t. For each formulation and measurement interval, the results were expressed as the mean ± standard deviation of three specimens.

The pH of the immersion medium was additionally recorded at the beginning and completion of the exposure period to assess changes in seawater conditions. The measured pH increased slightly from 7.9 before immersion to 8.3 after 960 h.

2.5. Thermal, Chemical, and Morphological Characterization

The melting and crystallization behavior of the investigated materials was characterized by differential scanning calorimetry (DSC) using a Mettler Toledo TGA/DSC2 STARe system (Mettler Toledo, Greifensee, Switzerland). Samples of approximately 10 mg were subjected to a heat–cool–heat cycle under a nitrogen atmosphere with a gas flow rate of supplied at 50 mL min^{-1}. The first heating scan was conducted from 25 to 300 °C, followed by cooling to 25 °C and a second heating to 300 °C. A constant scanning rate of 10 °C min^{-1} was applied throughout all three stages. To minimize the influence of processing-induced thermal history, the melting temperature (T_m) and melting enthalpy (ΔH_m) were obtained from the second heating scan.

Thermal degradation characteristics were investigated by thermogravimetric analysis using a Seiko Exstar TG/DTA 6300 analyzer (Seiko Instruments, Chiba, Japan). Approximately 10 mg of material was placed in the analyzer and heated from ambient temperature to 800 °C at 10 °C min^{-1} under a nitrogen atmosphere maintained at 50 mL min^{-1}. The mass-loss profiles were subsequently examined to compare the degradation behavior and thermal stability of the rPP/PCP formulations.

Chemical characteristics of the materials were examined by Fourier-transform infrared (FTIR) spectroscopy using a PerkinElmer Spectrum 100 spectrometer (PerkinElmer, Waltham, MA, USA). Spectra were collected between 4000 and 400 cm^{-1}. The resulting absorption bands were evaluated to identify the characteristic chemical functionalities of rPP and PCP and to examine spectral variations associated with the incorporation of PCP into the polymer matrix.

Morphological observations were carried out on the fractured surfaces of specimens obtained after impact testing. A Zeiss EVO LS10 scanning electron microscope (Zeiss, Oberkochen, Germany) was used to examine the distribution of PCP particles within the rPP matrix and the characteristics of the filler–matrix interface. Particular attention was given to features such as interfacial separation, particle pull-out, voids, and fracture patterns. Before imaging, the fracture surfaces were coated with an approximately 100 Å thick gold

layer to improve surface conductivity. SEM observations were performed at an accelerating voltage of 20 kV.

2.6. Statistical Analysis

Experimental results are reported as mean ± standard deviation. Statistical differences among the formulations were evaluated by one-way analysis of variance (ANOVA) using Minitab 17 statistical software (Minitab Inc., State College, PA, USA). When a significant effect was identified, Tukey's honestly significant difference (HSD) test was applied for multiple comparisons. Differences were considered statistically significant at $p < 0.05$. In the corresponding tables, mean values followed by different superscript letters within the same column indicate statistically significant differences ($p < 0.05$).

3. Results

3.1. Chemical Composition of Arceuthos drupacea Cone Powder

The chemical composition of *Arceuthos drupacea* cone powder was determined to evaluate its lignocellulosic constituents. The filler contained 36.36 ± 1.20 wt.% cellulose, 11.55 ± 0.30 wt.% hemicellulose, 34.20 ± 0.60 wt.% lignin, 9.35 ± 0.50 wt.% ash, and 8.54 ± 1.00 wt.% extractives. The cellulose content was calculated indirectly using a mass-balance approach. The calculated holocellulose content, representing the combined cellulose and hemicellulose fractions, was 47.91 wt.%. These results indicate that PCP contains substantial cellulose and lignin fractions, which may influence its interfacial interactions with the recycled polymer matrix and the resulting composite properties. In particular, the hydroxyl-containing polysaccharide fractions may contribute to moisture affinity and interfacial interactions, whereas the lignin-rich fraction may influence the thermal degradation behavior of the filler. However, the extent of these contributions cannot be determined from chemical composition data alone.

Compared with the species-specific composition reported by Dönmez et al. [18], the present PCP exhibited a higher calculated holocellulose content and a slightly higher lignin content. These differences may be associated with natural variability in the collected material and differences in analytical procedures. However, the indirectly calculated cellulose content should not be considered directly equivalent to the experimentally determined α-cellulose fraction reported in the literature. Furthermore, the calculated holocellulose content should be interpreted with caution when compared with values obtained using direct chemical isolation methods.

3.2. Mechanical Properties

The tensile properties of the rPP control and rPP/PCP composites are presented in Table 2 and Figure 2. PCP content had a significant effect on the tensile behavior of rPP ($p < 0.05$). The elastic modulus increased from 441.06 ± 16.14 MPa for the rPP control to 459.32 ± 49.76, 516.94 ± 36.53, and 549.23 ± 36.81 MPa for rPP-PCP5, rPP-PCP10, and rPP-PCP15, respectively. Thus, the maximum modulus obtained at 15 wt.% PCP represented an increase of approximately 24.5% relative to the control. At 20 wt.% PCP, the modulus decreased slightly to 508.81 ± 14.70 MPa but remained approximately 15.4% higher than that of the control. According to Tukey's HSD test, rPP-PCP10, rPP-PCP15, and rPP-PCP20 exhibited significantly higher modulus values than the control, whereas rPP-PCP5 was not statistically different from the control. The overall increase in stiffness is consistent with the presence of rigid lignocellulosic particles that restrict matrix deformation. However, because the PCP-containing formulations also included PP-g-MA, the observed improvement relative to the unfilled control cannot be attributed exclusively to PCP reinforcement. Similar

stiffening effects have been reported for pine-cone-reinforced PP systems [11] and other lignocellulosic-filled recycled PP composites [15].

Table 2. Tensile and flexural properties of the rPP control and rPP/PCP composites.

Sample Codes	Elastic Modulus (MPa)	Tensile Strength (MPa)	Elongation at Break (%)	Flexural Modulus (MPa)	Flexural Strength (MPa)
rPP (control)	441 ± 16.1 ^{c}	15.65 ± 0.1 ^{c}	93.9 ± 8.5 ^{a}	482 ± 27.6 ^{d}	11.15 ± 0.09 ^{e}
rPP-PCP5	459 ± 49.7 ^{bc}	16.13 ± 0.1 ^{b}	53.3 ± 5.7 ^{b}	564 ± 26.4 ^{c}	12.46 ± 0.12 ^{d}
rPP -PCP10	517 ± 36.5 ^{ab}	16.30 ± 0.3 ^{b}	34.8 ± 4.2 ^{c}	629 ± 19.9 ^{b}	13.73 ± 0.13 ^{c}
rPP -PCP15	549 ± 36.8 ^{a}	16.16 ± 0.3 ^{b}	42.3 ± 4.9 ^{c}	666 ± 19.6 ^{b}	14.34 ± 0.07 ^{b}
rPP -PCP20	509 ± 14.7 ^{ab}	16.63 ± 0.1 ^{a}	19.5 ± 2.4 ^{d}	720 ± 21.7 ^{a}	15.47 ± 0.09 ^{a}

Note: Values are expressed as mean ± standard deviation ($n = 5$). Different superscript letters within the same column indicate statistically significant differences according to one-way ANOVA followed by Tukey's HSD test ($p < 0.05$).

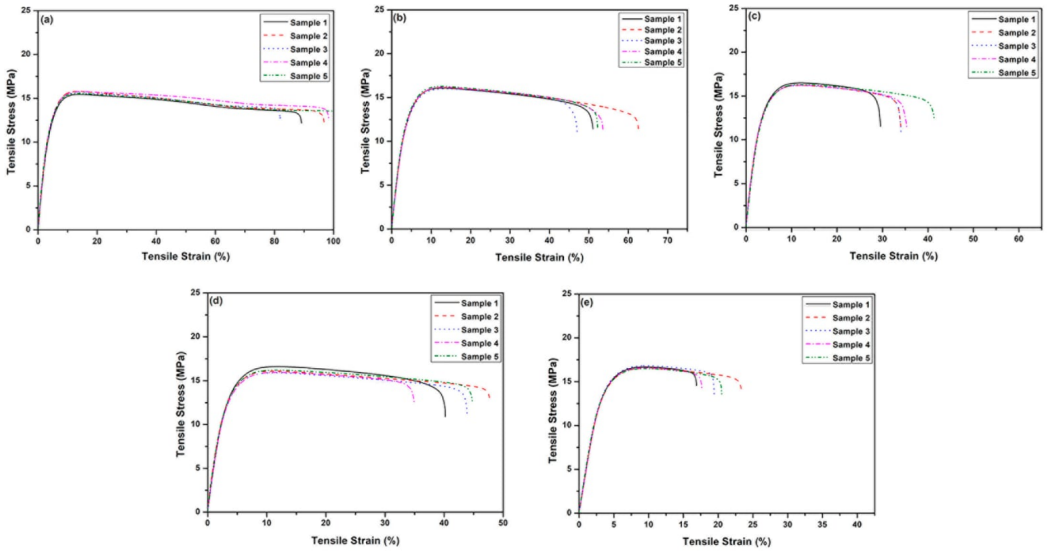

Figure 2. Tensile stress–strain curves of (**a**) rPP control, (**b**) rPP-PCP5, (**c**) rPP-PCP10, (**d**) rPP-PCP15, and (**e**) rPP-PCP20 composites.

Tensile strength was also significantly affected by the formulation ($p < 0.05$), although the magnitude of the changes was smaller than that observed for the elastic modulus. The tensile strength increased from 15.65 ± 0.14 MPa for the rPP control to 16.14 ± 0.10, 16.30 ± 0.13, and 16.16 ± 0.28 MPa for rPP-PCP5, rPP-PCP10, and rPP-PCP15, respectively. The highest value of 16.62 ± 0.13 MPa was obtained for rPP-PCP20, corresponding to an approximately 6.2% increase compared with the control. All PCP-containing formulations exhibited significantly higher tensile strength than the rPP control. No significant differences were observed among rPP-PCP5, rPP-PCP10, and rPP-PCP15, whereas rPP-PCP20 showed a significantly higher value than these three formulations. The preservation and moderate enhancement of tensile strength despite the replacement of up to 20 wt.% of rPP with PCP indicate that the compatibilized PCP-containing formulations maintained tensile load-bearing capacity. This response may reflect the combined contributions of PCP particles and PP-g-MA-mediated interfacial interactions, although their individual effects cannot be quantified using the present experimental design.

The presence of 3 wt.% PP-g-MA in all PCP-containing formulations likely contributed to maintaining effective stress transfer across the filler–matrix interface. Maleic-anhydride-grafted polypropylene can improve compatibility between non-polar PP and hydroxyl-

containing lignocellulosic surfaces, thereby promoting interfacial adhesion and mechanical stress transfer [15,17,29]. Kabache et al. [17], in particular, reported improved interfacial stress transfer associated with PP-g-MA in a pine-cone-flour-containing PP-based system. Nevertheless, because the present experimental design did not include PCP-containing formulations without PP-g-MA, the specific contribution of the compatibilizer cannot be quantitatively separated from the effect of PCP.

The present tensile-strength response can also be compared directly with the rPP/PCP system investigated by Do et al. [2]. They reported improved tensile performance following PCP incorporation, including an approximately 22% increase in tensile strength at 15 wt.% PCP. At a higher PCP concentration, however, the mechanical benefit diminished, which was associated with excessive filler concentration, agglomeration, and less efficient stress distribution [2]. In the present study, tensile strength remained above that of the control throughout the investigated PCP range and reached its highest value at 20 wt.% PCP. Differences in particle size, recycled-polymer characteristics, processing conditions, and compatibilization strategy may account for the different concentration-dependent responses between the studies.

A slight decline in elastic modulus from rPP-PCP15 to rPP-PCP20 suggests that the stiffening efficiency of PCP did not continue to increase proportionally at the highest filler loading. At elevated lignocellulosic filler contents, increased particle–particle interactions and deterioration in dispersion can reduce the efficiency of stress transfer. Kabache et al. [17] similarly reported poorer dispersion and the development of stress-concentration regions with increasing pine cone flour content. Their results further indicated that increasing PCF from 10 to 20–30 wt.% could restrict polymer-chain mobility and reduce some of the beneficial effects observed at lower filler loading. The relatively small reduction in modulus at 20 wt.% PCP in the present study may therefore reflect the onset of such concentration-dependent effects, although confirmation requires consideration of the corresponding morphological observations.

The most pronounced change in tensile behavior was observed for elongation at break. The rPP control exhibited an elongation of 93.91 ± 8.47%, which decreased significantly to 53.27 ± 5.75% after the incorporation of 5 wt.% PCP. Values of 34.85 ± 4.23% and 42.27 ± 4.93% were obtained for rPP-PCP10 and rPP-PCP15, respectively, with no statistically significant difference between these two formulations. At 20 wt.% PCP, elongation decreased further to 19.54 ± 2.54%, corresponding to an approximately 79.2% reduction relative to the control. The substantial loss in deformability is consistent with the presence of rigid lignocellulosic particles that constrain polymer-chain mobility and reduce the ability of the rPP matrix to undergo extensive plastic deformation. In addition, filler–matrix interfaces can act as local stress-concentration sites and facilitate earlier fracture as filler concentration increases [11,17]. Kabache et al. [17] likewise associated poor dispersion of untreated pine cone particles with stress-concentration regions capable of promoting fracture initiation.

Overall, the PP-g-MA-compatibilized PCP-containing formulations exhibited higher stiffness and moderately improved tensile strength, but substantially lower ductility, compared with the unfilled rPP control. The highest elastic modulus was obtained at 15 wt.% PCP, whereas rPP-PCP20 exhibited the highest tensile strength together with the lowest elongation at break. These findings demonstrate a clear stiffness–ductility trade-off and indicate that the appropriate PCP concentration should be selected according to the balance of stiffness, strength, and deformability required for the intended application.

The flexural properties of the rPP control and rPP/PCP composites are presented in Table 2 and Figure 3. PCP incorporation resulted in a progressive improvement in flexural performance. The flexural modulus increased from 482 ± 27.6 MPa for the rPP control to

564 ± 26.4, 629 ± 19.9, 666 ± 19.6, and 720 ± 21.7 MPa for rPP-PCP5, rPP-PCP10, rPP-PCP15, and rPP-PCP20, respectively. The maximum value obtained at 20 wt.% PCP corresponded to an increase of approximately 49.4% relative to the control. According to Tukey's HSD test, rPP-PCP10 and rPP-PCP15 were statistically comparable, whereas the other groups showed significant differences ($p < 0.05$). Flexural strength exhibited an even more systematic increase, rising from 11.15 ± 0.09 MPa for the control to 15.47 ± 0.09 MPa at 20 wt.% PCP, corresponding to an improvement of approximately 38.7%. All formulations were significantly different from one another ($p < 0.05$). The closely overlapping replicate curves in Figure 3 are also consistent with the relatively low experimental variability, particularly in flexural strength.

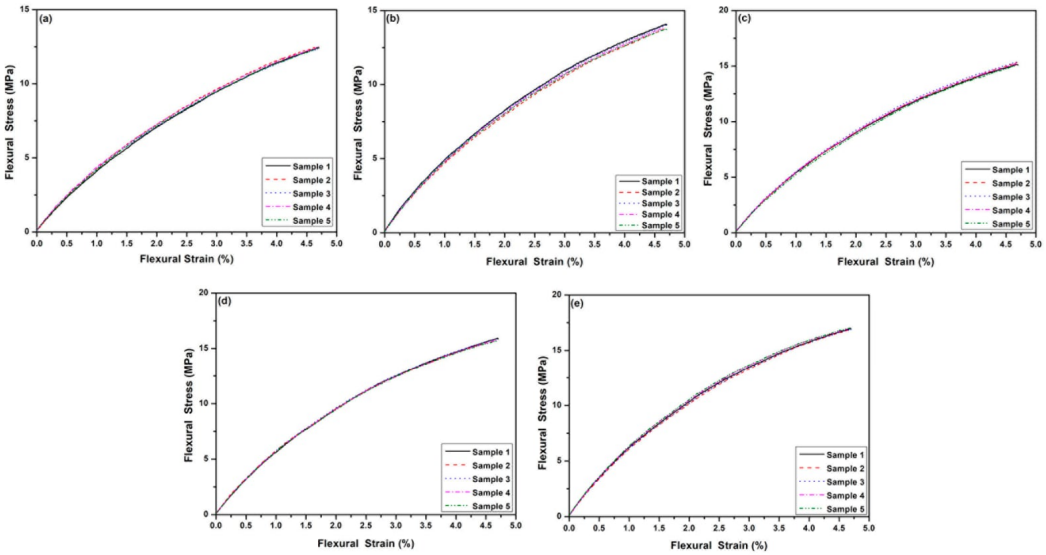

Figure 3. Flexural stress–strain curves of (**a**) rPP control, (**b**) rPP-PCP5, (**c**) rPP-PCP10, (**d**) rPP-PCP15, and (**e**) rPP-PCP20 composites.

The progressive increase in flexural modulus among the PCP-containing formulations is consistent with the increasing proportion of rigid lignocellulosic particles under a constant PP-g-MA concentration. These particles may restrict local deformation of the polymer matrix under bending, thereby contributing to the observed increase in stiffness. However, the respective contributions of particle reinforcement and matrix deformation constraint cannot be independently quantified from the present mechanical measurements. However, the improvements relative to the unfilled rPP control represent the overall response of the compatibilized composite formulations and cannot be attributed solely to PCP incorporation. Similar behavior has been reported for PP composites containing pine-derived particles. Maziero et al. [30] observed increasing flexural modulus with increasing Pinus particle content and associated this response with the higher stiffness of the dispersed lignocellulosic phase and its restriction of polymer deformation. Likewise, Atay and Türkmen [29] reported increasing flexural modulus with pine flour loading in PP composites containing 3 wt.% MAPP. Although the absolute values differ because of differences in matrix, filler characteristics, and processing conditions, these findings support the progressive stiffening observed in the present rPP/PCP system.

Notably, the increase in stiffness was accompanied by a continuous improvement in flexural strength up to 20 wt.% PCP, indicating that the higher filler content did not cause a deterioration in bending performance within the investigated range. This behavior is consistent with the direct rPP/PCP study of Do et al. [2], who also reported improved flexural properties following PCP incorporation. The presence of 3 wt.% PP-g-MA in the PCP-containing formulations may have contributed to effective load transfer by promoting

compatibility between the lignocellulosic surface and the PP matrix. Improved matrix–particle adhesion and stress transfer in maleated PP/Pinus systems have also been reported by Maziero et al. [30]. Nevertheless, the SEM observations of interfacial gaps and particle pull-out cavities suggest that interfacial adhesion was not uniformly effective, indicating that localized debonding and stress concentrations may coexist with the observed improvement in flexural properties. However, because the present study did not include PCP-filled formulations without PP-g-MA, the individual contribution of the compatibilizer cannot be separated from the reinforcing effect of PCP.

Overall, the flexural results demonstrate a pronounced improvement in the flexural performance of the compatibilized rPP/PCP formulations, with the highest flexural modulus and strength obtained at 20 wt.% PCP. Together with the tensile results, these findings reveal a characteristic stiffness–ductility trade-off: increasing PCP content substantially enhanced resistance to tensile and flexural deformation while reducing tensile elongation. The morphological observations discussed subsequently provide further insight into the filler distribution and interfacial characteristics associated with these mechanical responses. Although the results are consistent with combined particle reinforcement, matrix deformation constraint, and possible interfacial stress transfer, the individual contributions of these mechanisms cannot be quantitatively distinguished using the available experimental evidence.

The concentration-dependent variations in tensile and flexural strength are compared in Figure 4. While tensile strength exhibited relatively modest changes across the investigated PCP concentrations, flexural strength increased progressively with increasing filler loading. At 20 wt.% PCP, tensile and flexural strengths were approximately 6.3% and 38.7% higher, respectively, than those of the unfilled rPP control. This comparison highlights the more pronounced improvement in flexural strength within the investigated composite formulations, while the corresponding standard deviations indicate the variability of the measured properties.

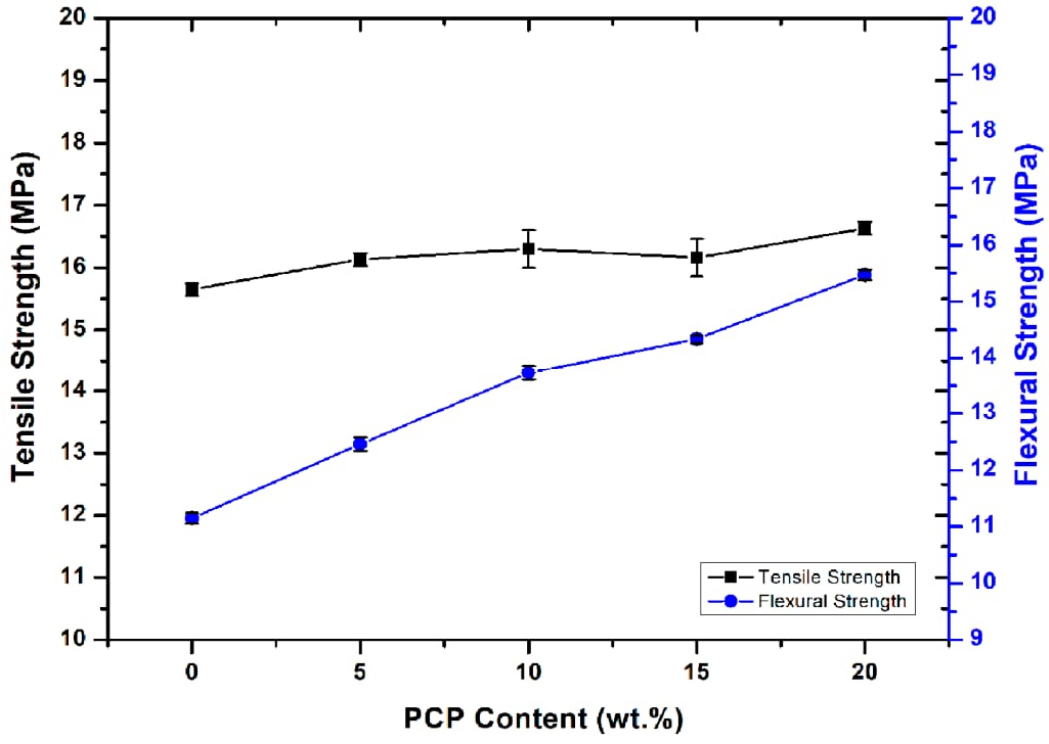

Figure 4. Effect of cone powder content on the tensile and flexural strengths of rPP/PCP composites. Error bars represent standard deviations ($n = 5$).

The notched Izod impact strength results of the rPP control and rPP/PCP composites are presented in Table 3 ang Figure 5. In contrast to the improvements observed in tensile and flexural stiffness, impact strength decreased progressively with increasing PCP content. The rPP control exhibited the highest impact strength of 21.60 ± 1.48 kJ/m^2, which decreased to 17.90 ± 0.57, 11.97 ± 1.29, 9.81 ± 0.50, and 8.82 ± 0.44 kJ/m^2 for rPP-PCP5, rPP-PCP10, rPP-PCP15, and rPP-PCP20, respectively. These values correspond to reductions of approximately 17.1%, 44.6%, 54.6%, and 59.2% relative to the control. One-way ANOVA revealed a significant effect of formulation on impact strength ($p < 0.001$). Tukey's HSD test indicated significant differences among most formulations ($p < 0.05$), whereas rPP-PCP15 and rPP-PCP20 exhibited statistically comparable impact resistance.

Table 3. Impact strength and hardness of the rPP control and rPP/PCP composites.

Sample Code	Notched Izod Impact Strength (kJ/m^2)	Hardness (Shore D)
rPP (control)	21.60 ± 1.48 ^{a}	58.10 ± 0.10 ^{e}
rPP-PCP5	17.90 ± 0.57 ^{b}	58.43 ± 0.15 ^{d}
rPP-PCP10	11.97 ± 1.29 ^{c}	59.10 ± 0.10 ^{c}
rPP-PCP15	9.81 ± 0.50 ^{d}	59.86 ± 0.12 ^{b}
rPP-PCP20	8.82 ± 0.44 ^{d}	60.45 ± 0.09 ^{a}

Note: Values are expressed as mean ± standard deviation ($n = 10$ for impact strength and $n = 5$ for Shore D hardness). Superscript letters (a–e) represent statistical groupings determined by one-way ANOVA followed by Tukey's HSD post hoc test. Within each column, values sharing the same superscript letter are not significantly different ($p \geq 0.05$), whereas values with different superscript letters differ significantly ($p < 0.05$).

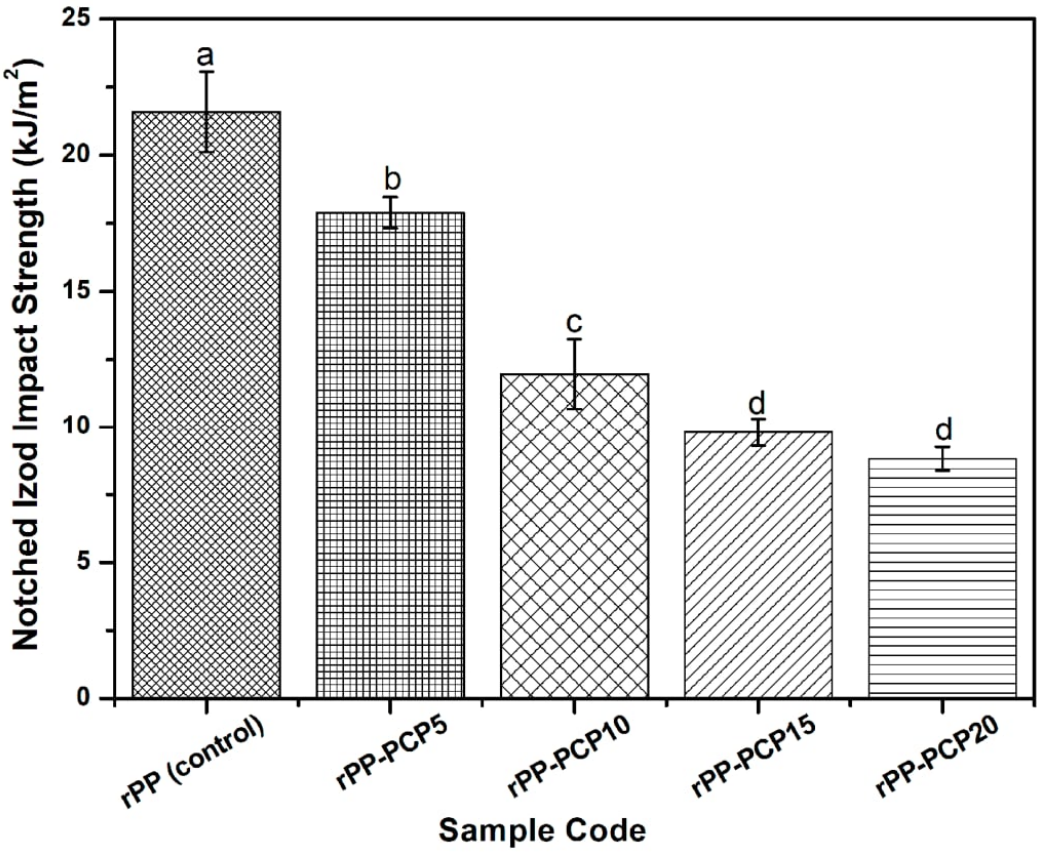

Figure 5. Effect of cone powder content on the notched Izod impact strength of rPP/PCP composites. Error bars represent standard deviations ($n = 10$). Different letters indicate statistically significant differences according to Tukey's HSD test ($p < 0.05$).

The reduction in impact strength may be associated with the increasing concentration of rigid lignocellulosic particles within the rPP matrix. Under impact loading, filler particles and their interfaces with the surrounding polymer can serve as stress-concentration regions, potentially facilitating crack initiation and propagation. In particular, locally clustered particles and interfacial discontinuities may promote stress localization and provide preferential sites for crack initiation, while particle–matrix debonding may facilitate subsequent crack propagation. Furthermore, increasing the PCP content reduces the relative proportion of the polymer phase available for plastic deformation and impact energy dissipation. These effects may explain why the improvements in tensile and flexural stiffness were accompanied by a substantial reduction in impact resistance. The concurrent decrease in tensile elongation further supports the development of a stiffer but less ductile mechanical response with increasing PCP loading.

The influence of pine-cone-derived reinforcement on impact performance, however, is not uniform across polypropylene-based composites. Do et al. [3] reported improved toughness and impact-related performance in recycled/virgin polypropylene blends containing PCP, which was associated with changes in crystallization behavior and microstructural characteristics. This contrasts with the continuous reduction in impact strength observed in the present study. Such differences may arise from variations in matrix composition, filler characteristics, processing conditions, and crystallization behavior. Similarly, Negi et al. [12] demonstrated that the impact performance of polypropylene composites reinforced with pine cone scale fibers and Vigna mungo powder depends on reinforcement composition and characteristics. These findings suggest that the contribution of pine-cone-derived materials to impact resistance is strongly formulation-dependent and cannot be generalized across different composite systems.

Although 3 wt.% PP-g-MA was incorporated into the PCP-containing formulations to promote interfacial compatibility, the impact strength decreased with increasing filler loading. This indicates that the presence of the compatibilizer was insufficient to maintain the impact resistance of the unfilled rPP control under the investigated conditions. Nevertheless, the specific contribution of PP-g-MA cannot be isolated because PCP-filled formulations without compatibilizer were not investigated. Overall, the results demonstrate a clear stiffness–toughness trade-off in the developed rPP/PCP composites. While higher PCP contents improved resistance to tensile and flexural deformation, they substantially reduced impact energy absorption. Consequently, the selection of PCP loading should consider the mechanical requirements of the intended application, particularly where resistance to sudden or localized impact loading is important.

The Shore D hardness results of the rPP control and rPP/PCP composites are presented in Table 3. Hardness increased progressively with PCP incorporation, from 58.10 ± 0.10 for the rPP control to 60.45 ± 0.09 for rPP-PCP20, corresponding to an improvement of approximately 4.0%. One-way ANOVA revealed a significant effect of PCP content on hardness ($p < 0.001$), while Tukey's HSD test confirmed significant differences among all formulations ($p < 0.05$). This improvement can be associated with the incorporation of rigid lignocellulosic particles, which restrict localized deformation of the polymer matrix and increase its resistance to indentation. Similar reinforcing effects of pine-cone-derived fillers on the mechanical properties of polypropylene composites have been reported by Arrakhiz et al. [11]. The observed hardness trend is also consistent with the increased tensile and flexural stiffness of the present composites.

3.3. FTIR Analysis

The FTIR spectra of cone powder, the rPP control, and rPP/PCP composites containing different PCP loadings are presented in Figure 6. The PCP spectrum exhibited a broad

absorption band centered at approximately 3260 cm^{-1}, corresponding to O–H stretching vibrations associated with hydroxyl groups in cellulose, hemicellulose, and lignin. The absorption bands near 2916 and 2850 cm^{-1} were attributed to aliphatic C–H stretching vibrations, whereas the band at approximately 1732 cm^{-1} was associated with C=O stretching of carbonyl-containing groups, including ester and acetyl functionalities in hemicellulose and lignin-related constituents. The band observed at 1606 cm^{-1} was assigned to aromatic skeletal vibrations of lignin, while the pronounced absorption features around 1051–1029 cm^{-1} were related to vibrations of the polysaccharide structure, including C–O and C–O–C bonds. These assignments agree well with the findings of Kumar et al. [9], who identified characteristic bands at approximately 3300, 2924, 1730, 1609, and 1031 cm^{-1} in pine-cone-derived materials. In particular, the close correspondence between the carbonyl, aromatic, and polysaccharide-related bands supports the lignocellulosic characteristics of the PCP used in the present study.

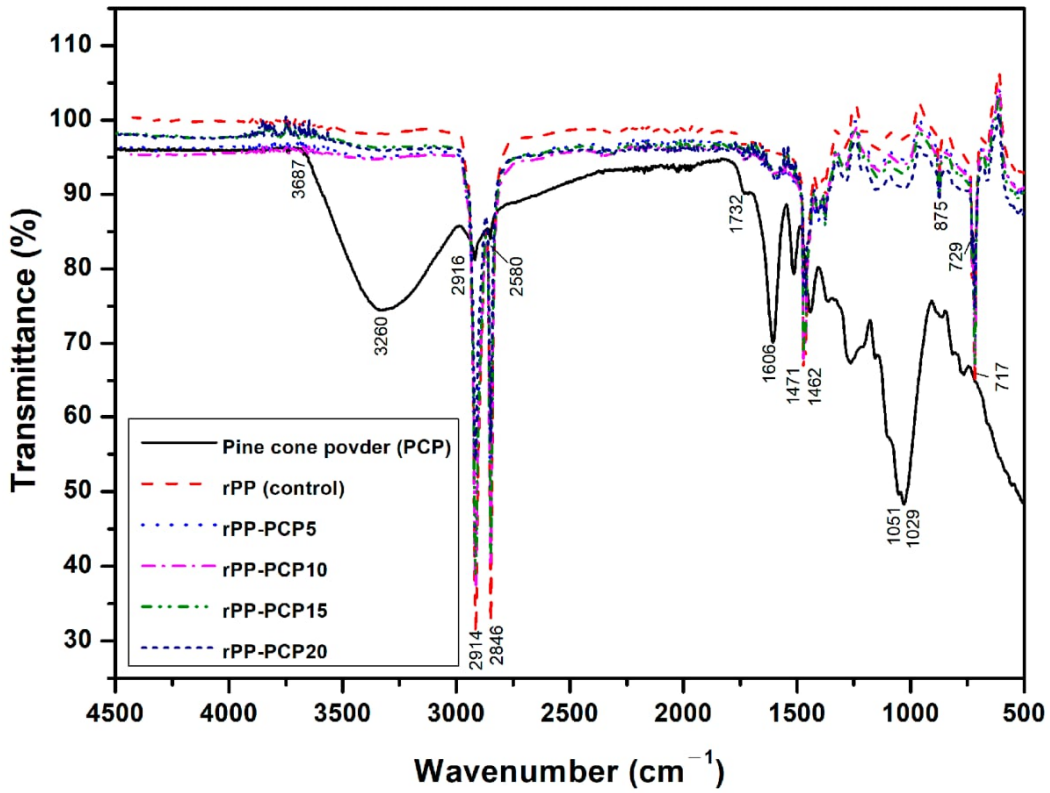

Figure 6. FTIR spectra of cone powder, the rPP control, and rPP/PCP composites containing different PCP loadings.

The FTIR spectrum of the rPP control was dominated by the characteristic absorption bands of polypropylene, particularly the intense aliphatic C–H stretching vibrations near 2914 and 2846 cm^{-1} and the deformation vibrations in the 1471–1462 cm^{-1} region. The rPP/PCP composites retained these principal spectral features across all investigated filler concentrations, indicating that the characteristic polypropylene vibrational bands remained detectable after melt compounding and injection molding. The overall similarity among the composite spectra also indicates that the spectral response was predominantly governed by the rPP matrix, despite the incorporation of increasing amounts of lignocellulosic filler. This behavior is consistent with the general chemical characteristics of polypropylene-based composites containing pine-derived lignocellulosic reinforcements [11,17].

Compared with the rPP control, the PCP-containing composites exhibited relatively subtle spectral differences, particularly in the regions associated with hydroxyl, carbonyl,

and polysaccharide-related vibrations. Although the broad O–H band was clearly distinguishable in the PCP spectrum, it was not readily resolved in the composite spectra. This may be associated with the relatively low contribution of PCP to the overall infrared response, overlapping spectral features, and the predominance of the polypropylene matrix. Similarly, the characteristic carbonyl and C–O-related bands of PCP were not sufficiently resolved to establish a systematic relationship between their intensities and filler concentration. The limited spectral differentiation among rPP-PCP5, rPP-PCP10, rPP-PCP15, and rPP-PCP20 therefore does not provide direct evidence of a progressive change in chemical bonding with increasing PCP loading.

The presence of hydroxyl and other oxygen-containing functional groups in PCP is relevant to its compatibility with the nonpolar polypropylene matrix. In the present study, 3 wt.% PP-g-MA was incorporated into all PCP-containing formulations to promote interfacial interactions between the lignocellulosic particles and rPP. Previous investigations involving pine-cone-derived fillers and polypropylene-based composites have highlighted the importance of compatibilization in determining composite performance [11,17]. However, the FTIR spectra obtained in the present study do not reveal sufficiently distinct new absorption bands or systematic peak shifts to confirm the formation of covalent bonds between PCP and PP-g-MA. Moreover, the carbonyl-containing groups naturally present in PCP may overlap with vibrations associated with the maleic anhydride functionality. Consequently, the possible contribution of PP-g-MA to interfacial adhesion cannot be established from FTIR analysis alone and should be evaluated in conjunction with the mechanical and morphological results.

Overall, the FTIR analysis identified the characteristic lignocellulosic functional groups of PCP and demonstrated the retention of the principal polypropylene absorption bands in the resulting composites. The close agreement between the PCP spectrum and the pine cone FTIR characteristics reported by Kumar et al. [9] supports the assignment of the main functional groups. Nevertheless, the substantial overlap among the composite spectra limits conclusions regarding filler-dependent chemical interactions. These findings provide a complementary chemical characterization of the investigated formulations, while the mechanical and morphological analyses offer further insight into the effects of PCP incorporation on composite performance.

3.4. Differential Scanning Calorimetry (DSC) Analysis

The differential scanning calorimetry (DSC) thermograms of the rPP control and rPP/PCP composites are presented in Figure 7, while the corresponding thermal parameters are summarized in Table 4. All formulations exhibited a dominant endothermic transition between 126.89 and 127.63 °C, accompanied by a considerably smaller melting event in the range of 160.25–162.68 °C. The presence of two distinguishable melting regions suggests that the recycled polymer matrix may contain crystalline polyolefin fractions with different thermal characteristics. Notably, the dominant melting temperature remained relatively unchanged with increasing PCP concentration, indicating that the incorporation of cone powder did not substantially alter the melting temperature of the principal crystalline fraction.

The dominant melting peak of the unfilled rPP control occurred at 127.63 °C, with a reported melting enthalpy of 140.17 J/g. Increasing the PCP concentration to 20 wt.% reduced the corresponding enthalpy to 100.18 J/g, representing an overall decrease of approximately 28.5%. However, this reduction should not be interpreted exclusively as a decrease in polymer crystallinity, since the progressive replacement of the polymer matrix by lignocellulosic filler inherently reduces the amount of crystallizable material per unit mass of composite. Furthermore, the relatively small variations in the dominant melting

temperature suggest that the principal thermal transition was largely preserved despite the increasing filler content. Previous investigations of lignocellulosic-filled polypropylene composites have similarly demonstrated that the incorporation of natural fillers may modify melting enthalpy and crystallization behavior without necessarily producing substantial changes in melting temperature [11,14,31,32]. The balance between heterogeneous nucleation and restrictions on polymer-chain mobility may contribute to such behavior, although these competing effects cannot be distinguished conclusively from the present heating thermograms alone.

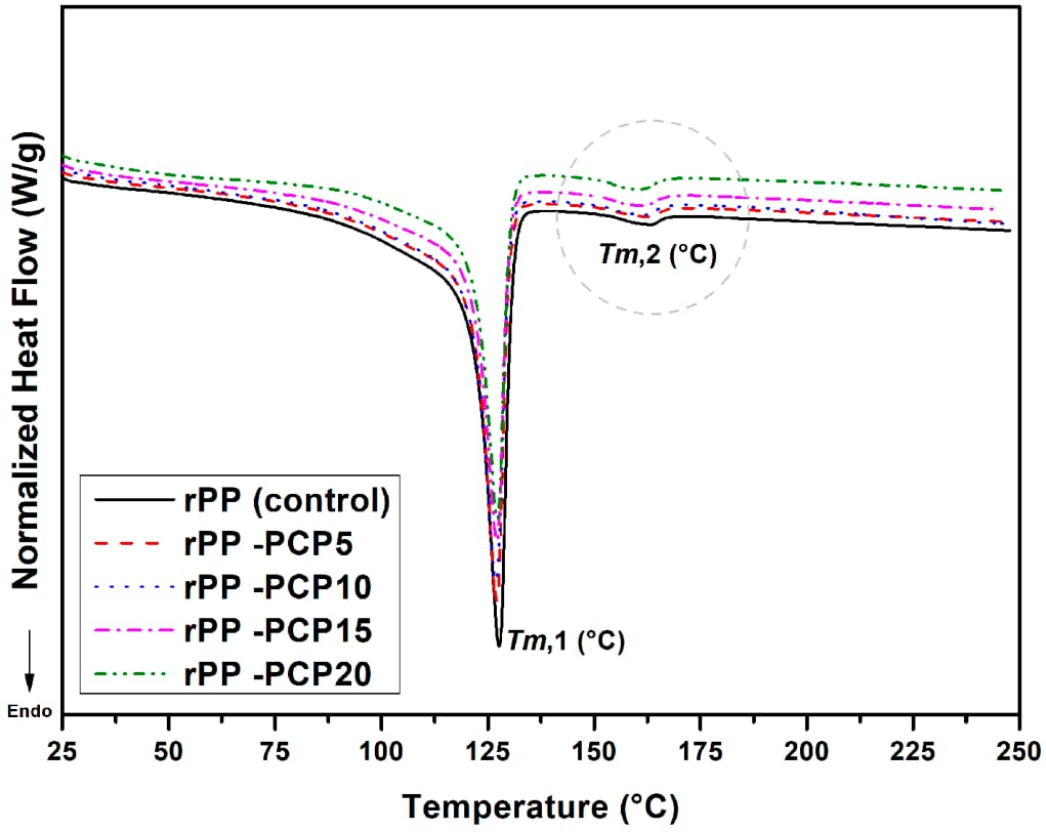

Figure 7. DSC heating thermograms of the rPP control and rPP/PCP composites, highlighting the dominant and secondary melting regions.

Table 4. DSC thermal parameters of the rPP control and rPP/PCP composites.

Sample Code	ΔHm,1 (J/g)	Tm,1 (°C)	ΔHm,2 (J/g)	Tm,2 (°C)
rPP (control)	140.17	127.63	2.64	162.68
rPP-PCP5	126.27	127.05	2.72	162.23
rPP-PCP10	126.84	126.89	2.95	160.88
rPP-PCP15	117.85	127.07	3.01	160.65
rPP-PCP20	100.18	127.22	3.09	160.25

Note: Tm,1 and Tm,2 denote the temperatures of the dominant and secondary melting peaks, respectively. ΔHm,1 represents the previously reported melting enthalpy, whereas ΔHm,2 is the approximate secondary-peak enthalpy obtained by baseline-corrected integration over 150–172 °C. The two enthalpy values should not be summed without confirming the original integration boundaries.

A particularly important feature of the present DSC results is the occurrence of a secondary endothermic peak near 160–163 °C. The secondary peak temperature decreased from approximately 162.68 °C for the rPP control to 160.25 °C for rPP-PCP20, while its estimated enthalpy varied between 2.64 and 3.09 J/g. This higher-temperature transition is consistent with the melting region commonly reported for polypropylene crystalline phases.

For example, Arrakhiz et al. [11] investigated pine cone fiber-reinforced polypropylene composites and reported melting behavior near 165 °C, while Kabache et al. [17] identified a polypropylene melting transition around 160 °C in PP-based composites containing pine cone flour. The comparatively low temperature of the dominant peak in the present study therefore differs substantially from the melting behavior typically associated with conventional isotactic polypropylene.

The coexistence of a dominant melting event near 127 °C and a smaller transition near 161–163 °C raises the possibility that the recycled polymer feedstock contains both polyethylene-like and polypropylene-like crystalline fractions. Such an interpretation is consistent with investigations of recycled polyolefin streams, where incomplete separation of PE and PP during recycling can result in materials exhibiting multiple melting transitions. Scoppio et al. [33] demonstrated that DSC can distinguish melting contributions associated with PE and PP in recycled polyolefin blends, although partial overlap between their melting regions complicates quantitative phase determination. Similarly, Kazmer et al. [34] discussed the characterization of industrial recycled polyolefins and the importance of identifying polymer cross-contamination, while Zhang et al. [35] reported composition-dependent thermal behavior in recycled PE/PP blends. Although highly crystalline HDPE typically exhibits melting temperatures approaching 135 °C, polyethylene melting behavior depends on molecular architecture, branching, and crystalline morphology. Therefore, the dominant transition near 127 °C remains compatible with polyethylene-like crystalline regions and does not exclude a polyethylene contribution. The melting behavior of propylene-based copolymers is strongly influenced by comonomer composition, with ethylene incorporation potentially reducing the melting temperature relative to conventional isotactic polypropylene [36,37]. In contrast, a melting transition near 127 °C is substantially below the characteristic melting range of conventional isotactic polypropylene, making an unmodified iPP homopolymer a less likely explanation for the dominant endotherm. Accordingly, the dominant endothermic transition near 127 °C cannot be unequivocally assigned to a polyethylene-rich fraction based on DSC measurements alone. However, the FTIR absorption bands at approximately 717 and 729 cm^{-1}, consistent with polyethylene-like crystalline sequences, suggest the possible presence of polyethylene-like crystalline domains within the recycled polymer matrix [38,39]. Nevertheless, the available thermal and spectroscopic evidence does not allow the precise chemical composition or relative proportions of the constituent polyolefin fractions to be conclusively established. Therefore, the proposed presence of different polyolefin fractions should be regarded as a plausible interpretation rather than definitive evidence of polyethylene contamination. Although previous recycling and thermal processing may influence polymer chain structure, crystallinity, and melting behavior, the present results do not provide sufficient evidence to attribute the occurrence of two distinct melting transitions directly to polymer degradation.

The contribution of the maleic anhydride-grafted polypropylene (PP-g-MA) compatibilizer must also be considered when interpreting the secondary melting event. The compatibilizer used in this study has a nominal melting temperature of approximately 162 °C and was incorporated at a constant concentration of 3 wt.% in the PCP-containing formulations. Consequently, PP-g-MA may contribute to the higher-temperature melting region of the composites. However, the observation of a corresponding peak in the uncompatibilized rPP control demonstrates that this transition cannot be attributed exclusively to the added PP-g-MA. Moreover, the slight increase in the estimated secondary-peak enthalpy with PCP loading should be interpreted cautiously because the relatively small peak partially overlaps with the high-temperature tail of the dominant melting transition, making the calculated enthalpy sensitive to baseline selection and integration limits.

The secondary melting temperature (Tm,2) decreased slightly from 162.68 °C for the unfilled rPP control to 160.25 °C for rPP-PCP20. This relatively small shift may reflect differences in the crystalline organization of the higher-melting polyolefin fraction, potentially associated with variations in lamellar thickness or crystal perfection. However, the available thermal data do not allow these structural contributions to be distinguished. In contrast, the apparent secondary melting enthalpy (ΔHm,2) increased from 2.64 to 3.09 J/g with increasing PCP loading. This increase does not necessarily indicate enhanced crystallinity, as the measured enthalpy represents the thermal response within the selected integration range rather than an independently resolved crystalline phase. Accordingly, the observed variations in Tm,2 and ΔHm,2 cannot be attributed unambiguously to PCP-induced crystallization or changes in crystalline perfection.

Overall, the DSC results indicate that increasing PCP content primarily reduced the measured dominant melting enthalpy while leaving the main melting temperature nearly unchanged. The secondary melting transition provides additional evidence of a thermally heterogeneous recycled polymer matrix, with possible contributions from polypropylene crystalline fractions and, in the compatibilized composites, PP-g-MA. Although previous studies have identified nucleating effects of pine cone-derived fillers in polypropylene systems [3], the present heating data do not provide sufficient evidence to establish a comparable nucleation mechanism. Since cooling crystallization thermograms were not available, the crystallization temperatures (Tc) and potential heterogeneous nucleation effects of PCP could not be directly evaluated. Furthermore, the uncertain composition of the recycled polyolefin matrix and the presence of multiple melting contributions prevented a reliable determination of absolute crystallinity using a single reference melting enthalpy. Consequently, the relationship between crystalline structure and mechanical performance could not be conclusively established from the available DSC data. Additional characterization, particularly polymer-specific FTIR analysis and DSC measurements of the recycled feedstock and neat PP-g-MA, would be valuable for resolving the origin of the two melting transitions and enabling a more reliable determination of phase-specific crystallinity.

3.5. Thermogravimetric Analysis (TGA)

The thermal degradation behavior of the recycled polypropylene (rPP) control and cone powder-filled composites was evaluated by thermogravimetric analysis under a nitrogen atmosphere. The TG and DTG curves are presented in Figures 8a and 8b, respectively, while the characteristic degradation temperatures and residual mass fractions are summarized in Table 5. All formulations exhibited a dominant mass-loss stage associated primarily with the thermal decomposition of the polyolefin matrix. Nevertheless, PCP incorporation produced noticeable differences in the initial mass-loss behavior and high-temperature residue, indicating that the lignocellulosic filler influenced the overall thermal response of the recycled polymer composites.

Table 5. Thermogravimetric analysis (TGA) parameters of the rPP control and rPP/PCP composites.

Sample Code	T5 (°C)	T50 (°C)	Tmax (°C)	Residue at 600 °C (%)	Residue at 800 °C (%)
rPP (control)	430.6	479.1	484.0	8.39	5.59
rPP-PCP5	368.9	480.8	485.0	7.34	3.84
rPP-PCP10	408.4	479.4	482.8	10.68	7.68
rPP-PCP15	347.0	477.8	482.8	10.76	6.52
rPP-PCP20	356.1	479.3	483.4	13.00	9.83

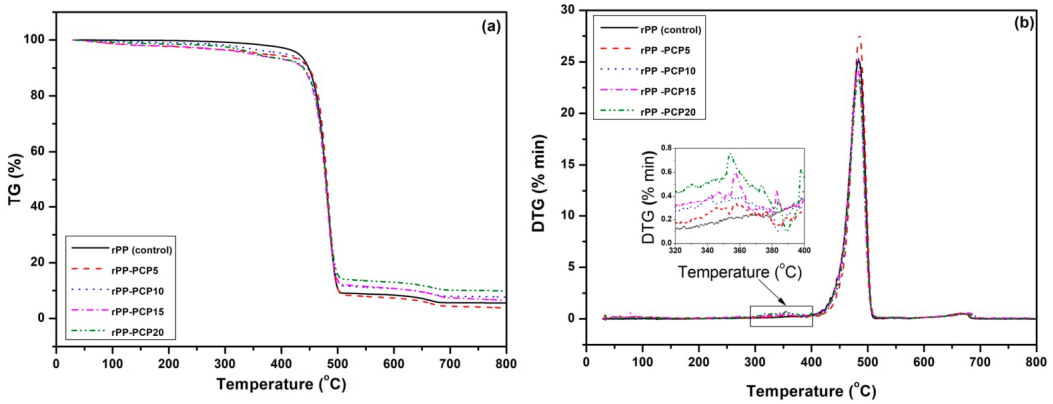

Figure 8. Thermogravimetric behavior of the rPP control and rPP/PCP composites under a nitrogen atmosphere: (**a**) thermogravimetric (TG) curves and (**b**) derivative thermogravimetric (DTG) curves.

The temperature corresponding to 5% mass loss (T_5) decreased from 430.6 °C for the unfilled rPP control to 368.9, 408.4, 347.0, and 356.1 °C for rPP-PCP5, rPP-PCP10, rPP-PCP15, and rPP-PCP20, respectively. The lowest T_5 was recorded for rPP-PCP15, corresponding to a reduction of 83.6 °C relative to the control. This pronounced reduction indicates a substantial deterioration in the initial thermal stability of the PCP-containing composites, despite the relatively unchanged T_{50} and T_{max} values. Consequently, the incorporation of PCP introduces a trade-off between the utilization of lignocellulosic waste as a reinforcing filler and the resistance of the composites to initial thermal degradation. This behavior is consistent with the incorporation of lignocellulosic constituents, including hemicellulose, cellulose, and lignin, which undergo thermal degradation over different temperature ranges. Similar reductions in initial degradation temperature have been reported for pine cone-filled polypropylene and polyethylene composites [11,40]. In particular, the pinecone-filled bio-based HDPE composites investigated in [40] exhibited a decrease in T_5 with increasing filler concentration, supporting the contribution of lignocellulosic constituents to early mass loss. Nevertheless, the T_5 values in the present study did not decrease monotonically with PCP content, as demonstrated by the comparatively higher value obtained for rPP-PCP10. This variation suggests that initial degradation behavior may also be influenced by filler heterogeneity, dispersion, and differences in the distribution of thermally labile constituents. Comparable complexities in the thermal response of natural-filler-reinforced recycled polypropylene systems have been discussed in previous studies [14,41].

Despite the pronounced changes in T_5, the temperature corresponding to 50% mass loss (T_{50}) remained within a narrow interval of 477.8–480.8 °C for all formulations. The unfilled rPP control exhibited a T_{50} of 479.1 °C, while the PCP-filled composites showed only minor deviations from this value. Similarly, the temperatures of maximum mass-loss rate (T_{max}), determined from the principal DTG peaks, ranged from 482.8 to 485.0 °C, compared with 484.0 °C for the control. These results indicate that PCP incorporation did not substantially shift the main thermal degradation stage, which remained predominantly associated with decomposition of the recycled polymer matrix. A comparable distinction between the onset of degradation and the principal mass-loss stage has been reported for lignocellulosic-filled polypropylene systems [11,41]. Furthermore, investigations involving pine cone and polypropylene during co-pyrolysis have demonstrated that the thermal degradation behavior of mixed lignocellulosic–polyolefin systems reflects contributions from components with different decomposition characteristics [42]. Accordingly, the relatively stable T_{50} and T_{max} values observed in the present study suggest that PCP primarily affected the earlier stages of mass loss rather than the temperature of maximum polymer degradation. However, the relatively unchanged main degradation temperatures should

not be interpreted as definitive evidence that the intrinsic thermal stability or degradation mechanism of the polymer matrix remained unaffected, since overlapping decomposition processes and potential filler–matrix interactions cannot be independently resolved from the present TGA measurements.

A minor DTG feature was observed around 350–360 °C, as illustrated in the magnified region of Figure 8b. Although a weak response was also present in the unfilled rPP control, the feature was more pronounced in some PCP-containing formulations. This behavior may partly reflect the thermal decomposition of lignocellulosic constituents introduced by PCP. Hemicellulose generally undergoes thermal degradation at relatively low temperatures, whereas cellulose decomposition occurs predominantly at higher temperatures, with additional overlapping contributions from lignin degradation. Therefore, the DTG response in this region may arise from overlapping decomposition processes rather than a single constituent. The presence of a weak signal in the unfilled control also suggests that the observed feature cannot be attributed exclusively to PCP decomposition. Compared with the dominant DTG peak near 480 °C, the substantially lower intensity of this feature indicates that it represents a minor thermal degradation event preceding the principal decomposition of the polyolefin matrix.

The residual mass measurements revealed further differences among the formulations. At 600 °C, the rPP control retained 8.39% of its initial mass, whereas rPP-PCP5, rPP-PCP10, rPP-PCP15, and rPP-PCP20 exhibited residual fractions of 7.34%, 10.68%, 10.76%, and 13.00%, respectively. At 800 °C, the corresponding values decreased to 5.59%, 3.84%, 7.68%, 6.52%, and 9.83%. The highest residual fraction was therefore obtained for rPP-PCP20, which retained 4.24 percentage points more mass than the unfilled control at 800 °C. The relatively greater residue at higher PCP loadings may be associated with carbonaceous char formation from lignocellulosic constituents and contributions from thermally persistent inorganic components. An increase in residual mass with pine cone filler content was also reported for bio-based HDPE composites [40], while studies on polypropylene composites containing natural reinforcements have highlighted the contribution of filler composition to thermal degradation and residue formation [14,31]. Nevertheless, the residue did not increase monotonically across the present formulations, and the appreciable residual mass of the unfilled control suggests that pre-existing constituents in the recycled polymer feedstock may also contribute. Therefore, the measured residue cannot be attributed exclusively to PCP-derived char.

An additional feature of the TG and DTG curves was a minor secondary mass-loss event at approximately 650–700 °C, following the principal degradation stage. The mass remaining between 600 and 800 °C decreased by 2.80, 3.50, 3.00, 4.24, and 3.17 percentage points for the control, rPP-PCP5, rPP-PCP10, rPP-PCP15, and rPP-PCP20, respectively. The presence of this secondary event in the unfilled control indicates that it cannot be attributed solely to PCP decomposition. Interestingly, previous characterization of commercial post-consumer polyethylene and polypropylene recyclates identified secondary high-temperature mass-loss events associated with the decomposition of inorganic constituents, particularly calcium carbonate [43]. This finding provides a plausible explanation for the behavior observed in the present recycled polymer formulations. Nevertheless, the presence of calcium carbonate or other specific inorganic compounds has not been independently confirmed in the current materials. Therefore, the secondary mass-loss event is interpreted cautiously as a possible contribution from residual inorganic constituents and/or further thermal transformations of carbonaceous residues rather than as definitive evidence of carbonate decomposition.

Overall, the TGA results demonstrate that PCP incorporation reduced the initial degradation temperature while leaving the characteristic temperatures of the main polymer decomposition stage largely unchanged. Higher PCP contents generally promoted greater

residual mass at elevated temperatures, although the response was not strictly proportional to filler loading. These findings are consistent with the complex thermal behavior reported for lignocellulosic-filled polyolefin composites [11,14,40–42]. The secondary mass-loss event further highlights the potential influence of residual constituents in recycled feedstocks, as discussed for commercial polyolefin recyclates [43]. Consequently, the thermal response of the developed composites should be considered the combined outcome of polymer-matrix degradation, lignocellulosic filler decomposition, formulation additives, and possible pre-existing constituents of the recycled material.

3.6. Seawater Absorption

The seawater absorption behavior of the recycled polypropylene (rPP) control and cone powder-filled composites was evaluated over an immersion period of 960 h (40 days), as illustrated in Figure 9. All formulations exhibited an overall increase in mass gain with immersion time, although the extent of seawater uptake was strongly dependent on PCP loading. The unfilled rPP control consistently exhibited the lowest absorption, whereas rPP-PCP20 showed the highest values. At the end of the immersion period, seawater absorption reached 0.2005%, 0.3628%, 0.6795%, 0.9312%, and 1.1356% for the rPP control, rPP-PCP5, rPP-PCP10, rPP-PCP15, and rPP-PCP20, respectively. Relative to the control, these values represent increases of approximately 81%, 239%, 364%, and 466% for the PCP-filled formulations. This filler-dependent behavior is consistent with the hydrophilic nature of lignocellulosic constituents, particularly cellulose and hemicellulose, whose hydroxyl groups facilitate interactions with water molecules. As discussed by Mohammed et al. [44], moisture uptake in natural-fiber-reinforced polymer composites is governed by the combined effects of reinforcement hydrophilicity, polymer–filler interfacial characteristics, and accessible transport pathways. Similarly, Tajvidi [45] investigated water uptake in natural-filler-reinforced polypropylene composites, providing a relevant basis for interpreting the increased moisture sensitivity observed with PCP incorporation.

The temporal evolution of seawater absorption revealed additional differences among the formulations. Extending the immersion period from 336 to 960 h revealed additional moisture uptake in all formulations. Notably, rPP-PCP15 and rPP-PCP20 exhibited further increases of approximately 17.3% and 19.7%, respectively, relative to their absorption values at 336 h, demonstrating that the shorter exposure period did not fully capture the subsequent moisture uptake behavior. The rPP control exhibited relatively limited mass gain and gradually approached a plateau of approximately 0.2005% toward the end of the 960 h exposure period. The rPP-PCP5 composite also showed a gradual reduction in its absorption rate, reaching approximately 0.3628% after 960 h. In contrast, the composites containing 10–20 wt.% PCP exhibited greater moisture uptake and required longer immersion periods to approach stabilization. Toward the end of the 960 h immersion period, the absorption curves exhibited a progressively decreasing rate of mass gain and approached an apparent plateau. However, the observed stabilization should not be regarded as definitive evidence of equilibrium moisture absorption without further assessment of measurement variability and longer-term exposure. Kahraman and Abu-Sharkh [46] examined palm-fiber-reinforced polypropylene composites exposed to distilled water and seawater and demonstrated that lignocellulosic reinforcement increased moisture uptake, with equilibrium behavior developing over substantially longer immersion periods. Although the filler type, concentration, and test conditions differed from those of the present study, their findings support the importance of distinguishing time-dependent moisture uptake from equilibrium absorption.

The influence of lignocellulosic filler concentration and immersion medium was further demonstrated by Kazemi Najafi and Younesi Kordkheili [47], who investigated wood

flour/polypropylene composites exposed to Caspian Sea water, Persian Gulf water, and distilled water. Their results indicated that higher wood flour contents increased water absorption, while exposure to Persian Gulf water produced greater mass gain and more pronounced deterioration in flexural properties than exposure to the other media. These observations highlight the importance of both reinforcement content and aqueous environmental conditions in determining the moisture response of natural-filler-reinforced polyolefin composites. Nevertheless, the considerably higher wood flour concentrations employed in that study and the differences in exposure conditions preclude direct quantitative comparison with the present results. Furthermore, because only seawater immersion was investigated in the current study, the specific contribution of salinity to the measured mass gain cannot be independently established.

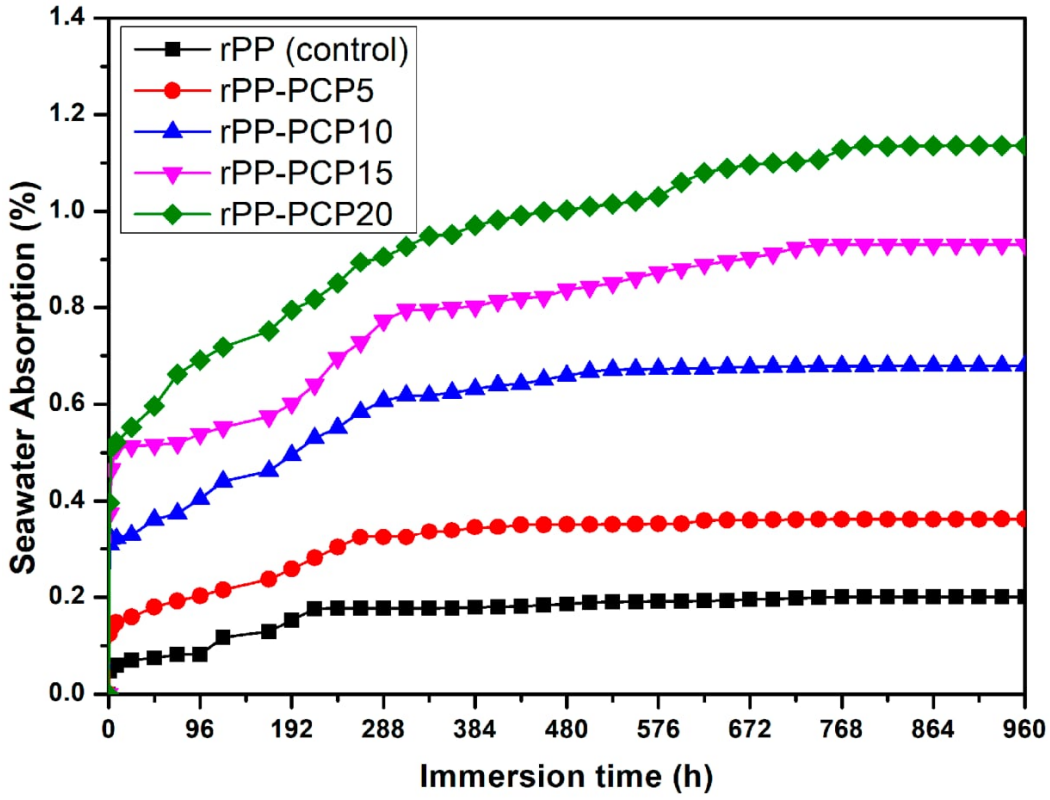

Figure 9. Seawater absorption behavior of the rPP control and rPP/PCP composites during 960 h (40 days) of immersion in natural seawater. Values represent the mean of three independently tested specimens ($n = 3$).

Beyond the intrinsic hydrophilicity of PCP, the polymer–filler interface may contribute to seawater penetration. Increasing filler content introduces additional interfacial regions that can potentially act as moisture transport pathways when particle encapsulation or interfacial adhesion is incomplete. The interfacial gaps, particle pull-out cavities, and locally clustered filler regions identified in the SEM analysis, where discernible, may contribute to localized moisture accumulation and facilitate water penetration. However, these observations do not establish continuous moisture transport pathways or allow the individual contributions of filler hydrophilicity and microstructural defects to be quantitatively distinguished. Moisture-induced swelling of lignocellulosic particles may also generate localized stresses and promote interfacial debonding during prolonged exposure. Fayzullin et al. [48] emphasized the relevance of natural-filler modification and interfacial characteristics to the water absorption behavior of polypropylene-based composites. In the present formulations, 3 wt.% maleic anhydride-grafted polypropylene (PP-g-MA) was incorporated into all PCP-

filled composites to promote compatibility between the nonpolar polymer matrix and the polar lignocellulosic filler. However, the presence of a compatibilizer does not necessarily eliminate moisture uptake associated with the reinforcement [46]. Moreover, because no PCP-filled formulation without PP-g-MA was included, the independent contribution of compatibilization to the measured seawater absorption cannot be determined. Accordingly, the observed increase in water uptake should be interpreted as the overall response of the investigated formulations rather than as an isolated effect of PCP or PP-g-MA.

Despite the pronounced relative increase in seawater absorption with PCP loading, the absolute mass gain remained below 1% for formulations containing up to 15 wt.% PCP after 960 h, whereas rPP-PCP20 reached approximately 1.14%. This finding indicates relatively low gravimetric moisture uptake during the 40-day immersion period, although it does not establish long-term moisture resistance. Importantly, the absorption results reveal a formulation-dependent trade-off when considered alongside the mechanical properties. The rPP-PCP20 composite exhibited the highest flexural modulus and flexural strength, but also the greatest seawater absorption and substantial reductions in impact strength and elongation at break relative to the unfilled control. Therefore, increasing PCP content improved stiffness and flexural load-bearing capacity under the tested conditions while simultaneously increasing moisture sensitivity and reducing deformation and impact tolerance. El Hawary et al. [49] highlighted the importance of environmental exposure and mechanical property retention when evaluating natural-fiber composites for marine applications. Furthermore, Fragassa et al. [50] discussed the challenges associated with water absorption and biological deterioration of natural-fiber composites in aquatic environments. In this context, the present findings demonstrate that cone powder derived from *Arceuthos drupacea* can be incorporated into recycled polypropylene, with the resulting composites exhibiting formulation-dependent seawater absorption over 40 days; however, the observed stabilization of moisture uptake does not establish long-term marine durability. Further investigations involving extended immersion, cyclic wetting–drying exposure, dimensional stability assessment, and post-immersion mechanical testing are required before the long-term suitability of these materials for marine components can be established.

3.7. Morphological Analysis

Scanning electron microscopy (SEM) was employed to examine the fracture-surface morphology of the rPP control and rPP/PCP composites, with particular emphasis on filler dispersion, polymer–filler interfacial characteristics, and microstructural features associated with mechanical failure. The incorporation of lignocellulosic particles into polypropylene can modify the fracture morphology through changes in local deformation behavior, stress transfer, and the development of interfacial discontinuities [2,11].

The fracture surface of the unfilled rPP control (Figure 10a) exhibited an irregular morphology characterized by localized deformation features and surface discontinuities. In the absence of PCP particles, these features are associated with deformation and fracture of the recycled polymer matrix itself. The comparatively high elongation at break (93.9%) and impact strength (21.60 kJ/m^2) of the control are consistent with its greater capacity to accommodate deformation before failure relative to the filled formulations.

The incorporation of PCP modified the fracture-surface morphology, introducing particle–matrix interfaces and additional sites at which localized stresses could develop (Figure 10b–d). The presence of embedded particles, interfacial gaps, particle pull-out cavities, and locally clustered filler regions, where identifiable in the micrographs, provides a morphological basis for evaluating the effectiveness of filler incorporation. These features suggest that particle dispersion and interfacial integrity may influence local stress distribution and fracture behavior. In particular, interfacial gaps and particle pull-out cavities are

consistent with localized debonding, which may facilitate crack initiation and propagation under impact loading. Similar features have been reported in pine cone–polypropylene composites, where particle dispersion and interfacial adhesion were identified as important factors governing mechanical performance [2,11]. Messaoudi et al. further demonstrated that interfacial contact in pine cone flour/PP composites can be influenced by surface modification and the incorporation of maleic anhydride-grafted polypropylene [51]. The importance of filler spatial organization has also been highlighted by Guo et al. [52] who investigated the influence of carbon fiber orientation on electrical transport and electromagnetic shielding performance in polymer composites. Although their study involves a different reinforcement geometry and focuses on functional rather than mechanical properties, it illustrates the broader role of filler architecture in determining composite behavior.

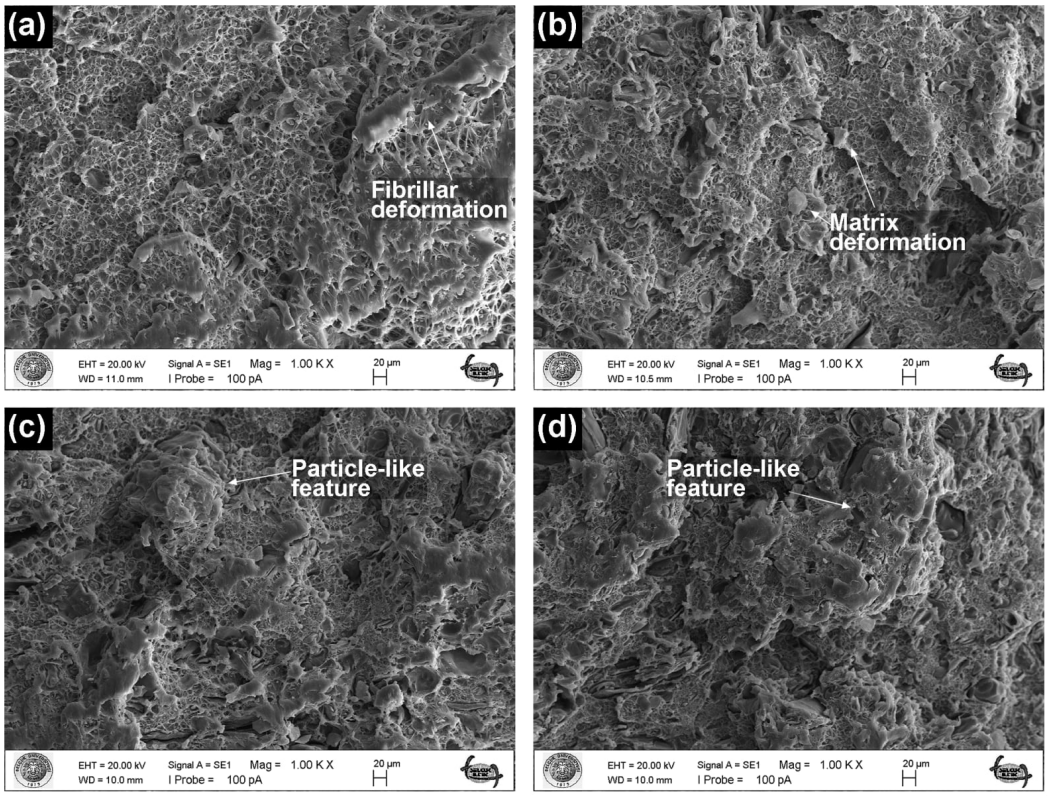

Figure 10. SEM micrographs of the impact-fractured surfaces of (**a**) rPP control, (**b**) rPP-PCP5, (**c**) rPP-PCP10, and (**d**) rPP-PCP20 composites at 1000× magnification.

The mechanical results indicate a progressive reduction in the ability of the composites to undergo deformation as PCP loading increased. Elongation at break decreased from 93.9% for the control to 53.3%, 34.8%, 42.3%, and 19.5% for PCP5, PCP10, PCP15, and PCP20, respectively. Likewise, impact strength decreased from 21.60 to 8.82 kJ/m^2 between the control and PCP20, corresponding to a reduction of approximately 59.2%. These changes suggest that increasing the concentration of relatively rigid lignocellulosic particles restricted matrix deformation and promoted more localized stress concentrations. Such behavior is consistent with the findings of Do et al. [2], who identified nonuniform particle distribution and interfacial debonding as relevant morphological features in recycled polypropylene composites containing cone powder. Nevertheless, the present SEM observations should be interpreted alongside the mechanical results rather than regarded as independent proof of a particular fracture mechanism.

In contrast to the reduction in ductility and impact resistance, the flexural modulus increased from 482 MPa for the control to 720 MPa for PCP20, while flexural strength

increased from 11.15 to 15.47 MPa. These improvements demonstrate the enhanced flexural performance of the PP-g-MA-compatibilized PCP-containing formulations relative to the unfilled rPP control, although the individual contributions of PCP and PP-g-MA cannot be distinguished. The simultaneous increase in stiffness and decrease in impact resistance is consistent with the general behavior reported for particulate lignocellulosic fillers in polypropylene matrices [11,53]. Notably, Do van et al. [3] reported improved toughness in a recycled polypropylene system containing cone powder. The difference from the present results highlights the importance of matrix composition, filler characteristics, formulation, and processing conditions in determining the balance between reinforcement and embrittlement.

All PCP-containing formulations included 3 wt% PP-g-MA, which was intended to promote compatibility between the hydrophobic rPP matrix and the polar lignocellulosic filler. Previous studies have shown that maleated polypropylene can improve interfacial contact and stress transfer in natural filler–polypropylene composites [51,54]. However, because the present experimental design did not include PCP-filled formulations without PP-g-MA, the individual contribution of the compatibilizer cannot be isolated from the overall formulation effect. Furthermore, morphological contact observed by SEM does not, by itself, establish the formation of covalent bonds at the polymer–filler interface.

Overall, the SEM analysis provides a complementary morphological framework for interpreting the mechanical performance of the rPP/PCP composites. The results indicate a trade-off between improved flexural performance and reduced deformation capacity as PCP content increased. For potential marine applications, the distribution of particles and the integrity of polymer–filler interfaces are particularly relevant because interfacial discontinuities may facilitate moisture penetration. This interpretation is consistent with the increase in short-term seawater absorption from 0.177% for the control to 0.949% for PCP20. However, the SEM observations alone cannot establish moisture-transport pathways or predict long-term durability under marine exposure.

4. Conclusions

This study investigated the potential of cone powder as a lignocellulosic filler for recycled polypropylene (rPP) composites, with particular emphasis on mechanical performance, thermal characteristics, fracture morphology, and seawater absorption over 960 h (40 days). The experimental results demonstrated that PCP incorporation substantially modified the performance of the recycled polymer system, providing improvements in flexural properties while introducing limitations associated with reduced toughness and increased moisture uptake.

The most pronounced improvements were observed in flexural performance. At 20 wt.% PCP, the flexural modulus increased from 482 to 720 MPa (49.4%), while flexural strength increased from 11.15 to 15.47 MPa (38.7%) relative to the unfilled control. Tensile strength also increased moderately, reaching 16.63 MPa, whereas the highest tensile modulus of 549 MPa was obtained at 15 wt.% PCP. These results demonstrate the effectiveness of the investigated PCP-containing formulations in improving stiffness and resistance to flexural deformation. However, impact strength decreased by 59.2% at 20 wt.% PCP, accompanied by a reduction in elongation at break from 93.9% to 19.5%. Therefore, higher filler contents improved load-bearing stiffness at the expense of deformation capacity and impact resistance.

FTIR analysis identified the characteristic chemical functionalities of PCP and the polymer matrix without providing unambiguous evidence of new covalent bond formation. DSC analysis revealed two melting regions, with a dominant transition near 127 °C and a secondary transition near 160–163 °C, reflecting the complex thermal behavior of the

recycled polymer system. TGA revealed a substantial reduction in initial thermal stability following PCP incorporation, with T_5 decreasing from 430.6 °C for the unfilled control to 347.0 °C for rPP-PCP15. Despite this pronounced decrease, T_{max} remained relatively stable (482.8–485.0 °C), indicating that PCP primarily affected the early stages of thermal degradation rather than the principal degradation stage. SEM observations further supported the mechanical findings by revealing changes in fracture-surface morphology and filler–matrix interfacial characteristics.

Immersion for 960 h (40 days) in natural seawater demonstrated a progressive increase in moisture uptake with increasing PCP concentration. After 960 h, seawater absorption increased from 0.2005% for the control to 1.1356% for the composite containing 20 wt.% PCP. Although seawater absorption remained below 1% for formulations containing up to 15 wt.% PCP, the composite containing 20 wt.% PCP exhibited greater moisture sensitivity. The absorption curves approached an apparent plateau toward the end of the immersion period; however, equilibrium moisture absorption could not be definitively established. Accordingly, the 960 h absorption results should not be interpreted as evidence of long-term seawater durability. Furthermore, post-immersion mechanical testing was not performed; therefore, the retention of mechanical properties following seawater exposure remains undetermined.

Overall, the findings demonstrate that *Arceuthos drupacea* cone powder can be incorporated into recycled polypropylene to develop composites with enhanced flexural properties and reduced reliance on polymer feedstock. Nevertheless, the substantial reductions in impact resistance and the increase in seawater absorption emphasize the importance of optimizing filler loading for the intended service conditions. For potential marine applications, these materials may be more appropriate for components where stiffness is prioritized over impact tolerance, provided that the relevant performance requirements are verified. Further investigations involving prolonged seawater immersion, cyclic environmental exposure, dimensional stability, and post-immersion mechanical testing are required to assess the long-term durability of these composites and establish their suitability for practical maritime applications.

Author Contributions: Conceptualization, İ.K., Ö.Ş. and M.Y.; methodology, İ.K., M.Y. and Ö.Ş.; validation, İ.K. and M.Y.; formal analysis, M.Y., Ö.Ş. and İ.K.; investigation, M.Y. and Ö.Ş.; resources, İ.K.; data curation, M.Y. and Ö.Ş.; writing—original draft preparation, M.Y. and Ö.Ş.; writing—review and editing, İ.K., M.Y. and Ö.Ş.; visualization, İ.K. and Ö.Ş.; project administration, Ö.Ş.; funding acquisition, Ö.Ş. and M.Y. All authors have read and agreed to the published version of the manuscript.

Funding: This research was supported by the Kocaeli University Scientific Research Projects Coordination Unit (BAP) under project number FBA-2026-5165 and the Yalova University Scientific Research Projects Coordination Unit (BAP) under project number 2024/ÖNAP/0012.

Institutional Review Board Statement: Not applicable.

Data Availability Statement: The data presented in this study are available on request from the corresponding author.

Acknowledgments: During the preparation of this manuscript, the authors used ChatGPT (GPT-5, OpenAI) to assist with language refinement and improve the clarity and organization of the manuscript. All AI-assisted content was critically reviewed and edited by the authors, who take full responsibility for the accuracy and integrity of the published work.

Conflicts of Interest: Author İdris Karagöz is the founder and a shareholder of Zamia Composite Research and Development Technology Joint Stock Company. The remaining authors declare no conflicts of interest. The funder had no role in the design of the study; the collection, analysis, or interpretation of data; the writing of the manuscript; or the decision to publish the results.

References

1. Yorulmaz, M.; Karabulut, K. Deniz Taşımacılığında Akıllı Gemiler: Gemi Kaptanlarının Bakış Açısı. *Ekon. İşletme Maliye Araştırmaları Derg.* **2021**, *3*, 40–54. [CrossRef]
2. Do, P.V.; Prabhakar, M.N.; Jayaraman, K.; Song, J.I. Biomass pinecone powder inclusion for mitigating mechanical degradation in recycled polypropylene extrusions. *Ind. Crops Prod.* **2024**, *222*, 119998. [CrossRef]
3. Do van, P.; Prabhakar, M.N.; Lee, D.W.; Li, M.; Song, J.I. Sustainable toughening of recycled polypropylene using pinecone powder as a bio-based nucleating agent. *Polym. Degrad. Stab.* **2025**, *237*, 111809. [CrossRef]
4. Srebrenkoska, V.; Bogoeva-Gaceva, G.; Avella, M.; Errico, M.E.; Gentile, G. Utilization of recycled polypropylene for production of eco-composites. *Polym.-Plast. Technol. Eng.* **2009**, *48*, 1113–1120. [CrossRef]
5. Homkhiew, C.; Ratanawilai, T.; Thongruang, W. Composites from recycled polypropylene and rubberwood flour: Effects of composition on mechanical properties. *J. Thermoplast. Compos. Mater.* **2015**, *28*, 179–194. [CrossRef]
6. Mohd Adnan, U.I.A.-B.; Wong, F.R.; Yong, S.K.; Morni, M.F.; Abdullah, A.H.; Rashid, A.A. Mechanical Properties of Rice Husk-Recycled Polypropylene Composite. *J. Mech. Eng.* **2023**, *12*, 45–61. [CrossRef]
7. Ibrahim, I.D.; Jamiru, T.; Sadiku, R.E.; Kupolati, W.K.; Agwuncha, S.C. Dependency of the Mechanical Properties of Sisal Fiber Reinforced Recycled Polypropylene Composites on Fiber Surface Treatment, Fiber Content and Nanoclay. *J. Polym. Environ.* **2017**, *25*, 427–434. [CrossRef]
8. Ardanuy, M.; Antunes, M.; Velasco, J.I. Vegetable fibres from agricultural residues as thermo-mechanical reinforcement in recycled polypropylene-based green foams. *Waste Manag.* **2012**, *32*, 256–263. [CrossRef] [PubMed]
9. Kumar, A.; Gupta, V.; Gaikwad, K.K. Microfibrillated cellulose from pine cone: Extraction, properties, and characterization. *Biomass Convers. Biorefin.* **2023**, *13*, 15413–15420. [CrossRef]
10. Kilic, A.; Hafizoglu, H.; Dönmez, I.E.; Tümen, I.; Sivrikaya, H.; Reunanen, M.; Hemming, J. Extractives in the cones of Pinus species. *Eur. J. Wood Wood Prod.* **2011**, *69*, 37–40. [CrossRef]
11. Arrakhiz, F.Z.; El Achaby, M.; Benmoussa, K.; Bouhfid, R.; Essassi, E.; Qaiss, A. Evaluation of mechanical and thermal properties of pine cone fibers reinforced compatibilized polypropylene. *Mater. Des.* **2012**, *40*, 528–535. [CrossRef]
12. Negi, R.S.; Prasad, L.; Yadav, A.; Winczek, J. Physical and Mechanical Properties of Pinecone Scale Fiber/Vigna Mungo Powder Reinforced Polypropylene Based Hybrid Composites. *J. Nat. Fibers* **2022**, *19*, 11458–11468. [CrossRef]
13. Dundar, T.; Ayrilmis, N.; Buyuksari, U. Utilization of Waste Pine Cone in Manufacture of Wood/Plastic Composite. In Proceedings of the Second International Conference on Sustainable Construction Materials and Technologies, Ancona, Italy, 28–30 June 2010; Volume 3, pp. 1517–1528, ISBN 978-1-4507-1490-7.
14. Andrzejewski, J.; Barczewski, M.; Szostak, M. Injection Molding of Highly Filled Polypropylene-based Biocomposites. Buckwheat Husk and Wood Flour Filler: A Comparison of Agricultural and Wood Industry Waste Utilization. *Polymers* **2019**, *11*, 1881. [CrossRef] [PubMed]
15. Morales, M.A.; Porras, J.; Maranon, A.; Casas, J.P.; Hernandez, C.; Michaud, V.; Porras, A. Effect of Polypropylene-Grafted-Maleic Anhydride and Rice Husk Particle Size on 3D-Printing Filament Composites From Recycled Polypropylene. *Polym. Compos.* **2025**, *46*, 15125–15141. [CrossRef]
16. Singh, M.K.; Arora, G.; Tewari, R.; Zafar, S.; Pathak, H.; Sehgal, A.K. Effect of pine cone filler particle size and treatment on the performance of recycled thermoplastics reinforced wood composites. *Mater. Today Proc.* **2022**, *62*, 7358–7363. [CrossRef]
17. Kabache, F.; Nekkaa, S.; Guessoum, M.; Aouissi, T.; Benayache, W. Assessment of various compatibilization methods effectiveness for upgrading properties of polypropylene/poly(lactic acid)/pine cone flour composites. *J. Adhes. Sci. Technol.* **2025**, *39*, 2334–2358. [CrossRef]
18. Dönmez, I.E.; Hafızoğlu, H.; Kılıç, A.; Tümen, İ.; Sivrikaya, H. Chemical composition of fourteen different coniferous species cones growing naturally in Turkey. *Wood Res.* **2012**, *57*, 339–344.
19. *Standard's ASTM D1102-84*; Standard Test Method for Ash in Wood. ASTM International: West Conshohocken, PA, USA, 2021. [CrossRef]
20. Li, S.; Xu, S.; Liu, S.; Yang, C.; Lu, Q. Fast pyrolysis of biomass in free-fall reactor for hydrogen-rich gas. *Fuel Process. Technol.* **2004**, *85*, 1201–1211. [CrossRef]
21. *Standard's ASTM D1106-21*; Standard Test Method for Acid-Insoluble Lignin in Wood. ASTM International: West Conshohocken, PA, USA, 2021. [CrossRef]
22. *Standard's TAPPI T 222*; om-21; Acid-Insoluble Lignin in Wood and Pulp. Technical Association of the Pulp and Paper Industry (TAPPI): Peachtree Corners, GA, USA, 2021.
23. Rowell, R.M. *Handbook of Wood Chemistry and Wood Composites*; CRC Press: Boca Raton, FL, USA, 2005.
24. Fengel, D.; Wegener, G. *Wood: Chemistry, Ultrastructure, Reactions*; Walter de Gruyter: Berlin, Germany, 2011.
25. *Standard's ISO 527-1:2019*; Plastics—Determination of Tensile Properties—Part 1: General Principles. International Organization for Standardization: Geneva, Switzerland, 2019.

26. *Standard's ISO 178:2019*; Plastics—Determination of Flexural Properties. International Organization for Standardization: Geneva, Switzerland, 2019.
27. *Standard's ISO 180:2023*; Plastics—Determination of Izod Impact Strength. International Organization for Standardization: Geneva, Switzerland, 2023.
28. *Standard's ISO 868:2003*; Plastics and Ebonite—Determination of Indentation Hardness by Means of a Durometer (Shore Hardness). International Organization for Standardization: Geneva, Switzerland, 2003.
29. Atay, H.Y.; Türkmen, M. Use of hornbeam, pine and MDF waste in wood-polymer composites as construction elements. *J. Indian Acad. Wood Sci.* **2022**, *19*, 110–120. [CrossRef]
30. Maziero, R.; Soares, K.; Filho, A.I.; Franco, A.R., Jr.; Rubio, J.C.C. Maleated polypropylene as coupling agent for polypropylene composites reinforced with eucalyptus and pinus particles. *BioResources* **2019**, *14*, 4774–4791. [CrossRef]
31. Karagöz, İ.; Büyükkaya, K.; Demirer, H.; Mudu, M.; Kartal, İ. Mechanical and thermal characterization of elastomer modified polypropylene hybrid composites reinforced with hazelnut shell and wollastonite fillers. *J. Appl. Polym. Sci.* **2024**, *141*, e55710. [CrossRef]
32. Karagöz, İ.; Duyar, H.İ.; Çavuşoğlu, A.; Sepetcioglu, H. Synergistic effects on the mechanical, thermal, and morphological properties of HDPE composites reinforced with Walnut Shell and Nano-Calcium Carbonate. *J. Appl. Polym. Sci.* **2025**, *142*, e57464. [CrossRef]
33. Scoppio, A.; Cavallo, D.; Müller, A.J.; Tranchida, D. Temperature modulated DSC for composition analysis of recycled polyolefin blends. *Polym. Test.* **2022**, *113*, 107656. [CrossRef]
34. Kazmer, D.O.; Nzeh, S.O.; Shen, B.; Elbert, D.C.; Nagarajan, R.; Sobkowicz-Kline, M.; Nguyen, T.D. Characterization, processing, and modeling of industrial recycled polyolefins. *Polym. Eng. Sci.* **2024**, *64*, 4801–4815. [CrossRef]
35. Zhang, W.; Shen, J.; Guo, X.; Wang, K.; Jia, J.; Zhao, J.; Zhang, J. Comprehensive Investigation into the Impact of Degradation of Recycled Polyethylene and Recycled Polypropylene on the Thermo-Mechanical Characteristics and Thermal Stability of Blends. *Molecules* **2024**, *29*, 4499. [CrossRef] [PubMed]
36. Papageorgiou, D.G.; Papageorgiou, G.Z.; Bikiaris, D.N.; Chrissafis, K. Crystallization and melting of propylene–ethylene random copolymers. Homogeneous nucleation and β-nucleating agents. *Eur. Polym. J.* **2013**, *49*, 1577–1590. [CrossRef]
37. Hu, Y.S.; Kamdar, A.R.; Ansems, P.; Chum, S.P.; Hiltner, A.; Baer, E. Crystallization of a miscible propylene/ethylene copolymer blend. *Polymer* **2006**, *47*, 6387–6397. [CrossRef]
38. Keller, A.; Sandeman, I. Investigation of unusual orientation in polyethylene by infrared spectroscopy. *J. Polym. Sci.* **1955**, *15*, 133–150. [CrossRef]
39. Kang, N.; Xu, Y.-Z.; Cai, Y.-L.; Li, W.-H.; Weng, S.-F.; Feng, W.; He, L.-T.; Xu, D.-F.; Wu, J.-G.; Xu, G.-X. Different states in orthorhombic crystalline phase of high-density polyethylene. *J. Mol. Struct.* **2001**, *562*, 19–24. [CrossRef]
40. Morcillo, M.D.C.; Tejada, R.; Lascano, D.; Garcia-Garcia, D.; Garcia-Sanoguera, D. Manufacturing and characterization of environmentally friendly wood plastic composites using pinecone as a filler into a bio-based high-density polyethylene matrix. *Polymers* **2021**, *13*, 4462. [CrossRef] [PubMed]
41. Wyderkiewicz, W.; Miedzianowska-Masłowska, J.; Sowińska-Baranowska, A.; Masłowski, M. Recycled Polypropylene Composites Reinforced with Microcellulose Fibres and Microcellulose-Derived Biochar: Thermal, Rheological and Mechanical Performance. *Materials* **2026**, *19*, 1942. [CrossRef] [PubMed]
42. Brebu, M.; Ucar, S.; Vasile, C.; Yanik, J. Co-pyrolysis of pine cone with synthetic polymers. *Fuel* **2010**, *89*, 1911–1918. [CrossRef]
43. Gall, M.; Freudenthaler, P.J.; Fischer, J.; Lang, R.W. Characterization of composition and structure–property relationships of commercial post-consumer polyethylene and polypropylene recyclates. *Polymers* **2021**, *13*, 1574. [CrossRef] [PubMed]
44. Mohammed, M.; Jawad, A.J.M.; Mohammed, A.M.; Oleiwi, J.K.; Adam, T.; Osman, A.F.; Dahham, O.S.; Betar, B.O.; Gopinath, S.C.B.; Jaafar, M. Challenges and advancement in water absorption of natural fiber-reinforced polymer composites. *Polym. Test.* **2023**, *124*, 108083. [CrossRef]
45. Tajvidi, M.; Ebrahimi, G. Water uptake and mechanical characteristics of natural filler–polypropylene composites. *J. Appl. Polym. Sci.* **2003**, *88*, 941–946. [CrossRef]
46. Kahraman, R.; Abu-Sharkh, B. Moisture absorption behavior of palm/polypropylene composites in distilled water and sea water. *Int. J. Polym. Mater.* **2007**, *56*, 43–53. [CrossRef]
47. Kazemi Najafi, S.; Younesi Kordkheili, H. Effect of sea water on water absorption and flexural properties of wood-polypropylene composites. *Eur. J. Wood Wood Prod.* **2011**, *69*, 553–556. [CrossRef]
48. Fayzullin, I.; Gorbachev, A.; Volfson, S.; Serikbayev, Y.; Nakyp, A.; Akylbekov, N. Composite material based on polypropylene and modified natural fillers. *Polymers* **2024**, *16*, 1703. [CrossRef] [PubMed]
49. El Hawary, O.; Boccarusso, L.; Ansell, M.P.; Durante, M.; Pinto, F. An overview of natural fiber composites for marine applications. *J. Mar. Sci. Eng.* **2023**, *11*, 1076. [CrossRef]
50. Fragassa, C.; Mattiello, S.; Fronduti, M.; Del Gobbo, J.; Gagic, R.; Santulli, C. Prevention of biofouling due to water absorption of natural fiber composites in the aquatic environment: A critical review. *J. Compos. Sci.* **2024**, *8*, 532. [CrossRef]

51. Messaoudi, K.; Nekkaa, S.; Guessoum, M. Contribution of surface treatments by esterification and silanization in reinforcing the composites based on Pine cone and Spartium junceum flours and polypropylene. *J. Adhes. Sci. Technol.* **2019**, *33*, 2405–2429. [CrossRef]
52. Guo, X.; Liang, D.; Li, Y.; Zhang, H.; Zheng, N.; Zhang, Y.; Zhao, T.; Zhang, Q.; Yin, M.; Zhao, Z.; et al. Orientation-tunable electromagnetic interference shielding in carbon fiber-based composites with semi-empirical modeling of anisotropic charge transport. *Carbon* **2026**, *252*, 121400. [CrossRef]
53. Ndiaye, D.; Matuana, L.M.; Morlat-Therias, S.; Vidal, L.; Tidjani, A.; Gardette, J.L. Thermal and Mechanical Properties of Polypropylene/Wood-Flour Composites. *J. Appl. Polym. Sci.* **2011**, *119*, 3321–3328. [CrossRef]
54. Stark, N.M.; Rowlands, R.E. Effects of wood fiber characteristics on mechanical properties of wood/polypropylene composites. *Wood Fiber Sci.* **2003**, *35*, 167–174.

Disclaimer/Publisher's Note: The statements, opinions and data contained in all publications are solely those of the individual author(s) and contributor(s) and not of MDPI and/or the editor(s). MDPI and/or the editor(s) disclaim responsibility for any injury to people or property resulting from any ideas, methods, instructions or products referred to in the content.